Research Paper

GEOSPHERE

GEOSPHERE, v. 20, no. 3

https://doi.org/10.1130/GES02709.1

11 figures; 2 tables; 1 set of supplemental files

CORRESPONDENCE: chapman@macalester.edu

CITATION: Chapman, A.D., Grischuk, J., Klapper, M., Schmidt, W., and LaMaskin, T., 2024, Middle Jurassic to Early Cretaceous orogenesis in the Klamath Mountains Province (Northern California–southern Oregon, USA) occurred by tectonic switching: Insights from detrital zircon U-Pb geochronology of the Condrey Mountain schist: Geosphere, v. 20, no. 3, p. 749–777, https://doi.org/10.1130/GES02709.1.

Science Editor: Christopher J. Spencer
Associate Editor: Andrew V. Zuza

Received 23 August 2023
Revision received 3 January 2024
Accepted 9 February 2024

Published online 12 April 2024

Middle Jurassic to Early Cretaceous orogenesis in the Klamath Mountains Province (Northern California–southern Oregon, USA) occurred by tectonic switching: Insights from detrital zircon U-Pb geochronology of the Condrey Mountain schist

Alan D. Chapman[1], Jennifer Grischuk[2], Meghan Klapper[3], William Schmidt[4], and Todd LaMaskin[5]

[1]Geology Department, Macalester College, Saint Paul, Minnesota 55105, USA
[2]Department of Geology and Geophysics, University of Wyoming, Laramie, Wyoming 82071, USA
[3]Metropolitan Council of the Twin Cities, Saint Paul, Minnesota 55101, USA
[4]Department of Earth Sciences, University of Southern California, Los Angeles, California 90089, USA
[5]Department of Earth and Ocean Sciences, University of North Carolina Wilmington, Wilmington, North Carolina 28403, USA

ABSTRACT

The Klamath Mountains Province of Northern California and southern Oregon, USA, consists of generally east-dipping terranes assembled via Paleozoic to Mesozoic subduction along the western margin of North America. The Klamath Mountains Province more than doubled in mass from Middle Jurassic to Early Cretaceous time, due to alternating episodes of extension (e.g., rifting and formation of the Josephine ophiolite) and shortening (e.g., Siskiyou and Nevadan events). However, the tectonic mechanisms driving this profound Mesozoic growth of the Klamath Mountains Province are poorly understood. In this paper, we show that formation of the Condrey Mountain schist (CMS) of the central Klamath Mountains Province spanned this critical time period and use the archive contained within the CMS as a key to deciphering the Mesozoic tectonics of the Klamath Mountains Province. Igneous samples from the outer CMS subunit yield U-Pb zircon ages of ca. 175–170 Ma, which reflect volcanic protolith eruptive timing. One detrital sample from the same subunit contains abundant (~54% of zircon grains analyzed) Middle Jurassic ages with Paleozoic and Proterozoic grains comprising the remainder and yields a maximum depositional age (MDA) of ca. 170 Ma. These ages, in the context of lithologic and thermochronologic relations, suggest that outer CMS protoliths accumulated in an outboard rift basin and subsequently underthrust the Klamath Mountains Province during the Late Jurassic Nevadan orogeny. Five samples of the chiefly metasedimentary inner CMS yield MDAs ranging from 160 Ma to 130 Ma, with younger ages corresponding to deeper structural levels. Such inverted age zonation is common in subduction complexes and, considering existing K-Ar ages, suggests that the inner CMS was assembled by progressive underplating over a >10 m.y. timespan. Despite this age zonation, age spectra derived from structurally shallow and deep portions of the inner CMS closely overlap those derived from the oldest section of the Franciscan subduction complex (South Fork Mountain schist). These relations suggest that the inner CMS is a composite of South Fork Mountain schist slices that were sequentially underplated beneath the Klamath Mountains Province. The age, inboard position, and structural position (i.e., the CMS resides directly beneath Jurassic arc assemblages with no intervening mantle) of the CMS suggest that these rocks were emplaced during one or more previously unrecognized episodes of shallow-angle subduction restricted to the Klamath Mountains Province. Furthermore, emplacement of the deepest portions of the CMS corresponds with the ca. 136 Ma termination of magmatism in the Klamath Mountains Province, which we relate to the disruption of asthenospheric flow during slab shallowing. The timing of shallow-angle subduction shortly precedes that of the westward translation of the Klamath Mountains Province relative to correlative rocks in the northern Sierra Nevada Range, which suggests that subduction dynamics were responsible for relocating the Klamath Mountains Province from the arc to the forearc. In aggregate, the above relations require at least three distinct phases of extension and/or rifting, each followed by an episode of shallow-angle underthrusting. The dynamic upper-plate deformation envisioned here is best interpreted in the context of tectonic switching, whereby slab steepening and trench retreat alternate with slab shallowing due to recurrent subduction of buoyant oceanic features.

Alan Chapman https://orcid.org/0000-0001-5937-2894

1. INTRODUCTION

Upper-plate domains of subduction zones are sites of significant arc magmatism, terrane accretion, tectonic underplating, tectonic erosion, delamination, and possibly relamination (e.g., Bird, 1979; von Huene and Lallemand, 1990; Davies and Stevenson, 1992; Stern and Scholl, 2010; Scholl and von Huene, 2009; Hacker et al., 2011; Jacobson et al., 2011). Mass flux calculations

involving these processes indicate that, compared with other tectonic settings, subduction zones are the biggest producers and destroyers of continental lithosphere on the planet (Cloos and Shreve, 1988; Kay and Mahlburg-Kay, 1991; von Huene and Scholl, 1991; Gutscher et al., 2000; Arndt, 2013).

Material fluxes to and from the overriding plate of a subduction zone are influenced by changes in the dip angle of the downgoing plate (Coney and Reynolds, 1977; Dewey, 1981; Collins, 2002; Brun and Faccenna, 2008; Schellart and Strak, 2021). For instance, sufficient shallowing of slab dip tends to inhibit arc magmatism via impingement of mantle-wedge corner flow, while promoting tectonic erosion through an increase in shear stress along the base of the upper plate (e.g., Saleeby, 2003). Furthermore, upper-plate shortening leads to mountain building and an increase in erosion; the resulting flood of detritus to the trench may drive significant accretion and/or tectonic underplating (e.g., Ducea et al., 2009). Conversely, steepening of a slab from a shallow trajectory (i.e., "slab rollback") may (re)ignite arc magmatism and lead to upper-plate extension and migration of the trench oceanward (e.g., Chapman et al., 2021). In particular, switching from shallow- to steep-angle subduction and vice versa appears to be an efficient net producer of continental crust (Collins, 2002).

In detail, upper-plate domains of modern subduction zones respond to changes in downgoing slab dip in diverse ways. For instance, magmatism in the Trans-Mexican Volcanic Belt has continued in spite of flat subduction of the Cocos plate beneath it, most likely due to slab melting plus nascent slab rollback and the associated influx of new asthenosphere (e.g., Ferrari et al., 2012). Furthermore, sufficient decoupling may result in a lower plate that glides into the mantle at low-dip with minimal upper-plate deformation, as appears to be the case along the Mexican flat slab (Pérez-Campos et al., 2008).

Recognition of ancient settings in which subduction trajectory varied is essential to understanding modern counterparts, as the geologic record permits investigation of the long-term (i.e., millions to tens of millions of years) effects of changes in slab dip over a range of crustal depths. The Pelona–Orocopia–Rand (and related) schists of Southern California represent an excellent example of such an archive of ancient slab shallowing followed by steepening (Grove et al., 2003; Jacobson et al., 2011; Chapman, 2017).

The Klamath Mountains Province of Northern California–southern Oregon, USA, apparently underwent rapid alternation between contraction and extension, most notably from Middle Jurassic to Early Cretaceous time (Saleeby et al., 1982; Harper and Wright, 1984; Wright and Wyld, 1986; Wright and Fahan, 1988; Hacker and Ernst, 1993; Harper et al., 1994; Hacker et al., 1995; Harper, 2003; Snoke and Barnes, 2006; Yule et al., 2006; LaMaskin et al., 2021; Surpless et al., 2024). Tectonic activity coincided with significant magmatic additions to the plate margin (Harper, 1984; Barnes et al., 1996; Allen and Barnes, 2006; Snoke and Barnes, 2006; Coint et al., 2013; Barnes and Barnes, 2020). The driving mechanisms behind tectonism and magmatism in the Klamath Mountains Province are controversial, with competing ideas ranging from global plate reorganization to collision of a large fragment of continental lithosphere (Schweickert and Cowan, 1975; Wernicke and Klepacki, 1988; Wright and Fahan, 1988; May et al., 1989; McClelland et al., 1992; Saleeby and Harper, 1993; Hacker et al., 1995; Wolf and Saleeby, 1995; Shervais et al., 2004; Seton et al., 2012; LaMaskin et al., 2021; Surpless et al., 2024). Both mechanisms predict extensive deformation over extended periods, yet observed contractional and extensional episodes were seemingly confined to a few hundred kilometers along the margin and occurred rapidly (in many cases, within less than 10 m.y. and often less than 5 m.y.). This paper contributes new U-Pb igneous and detrital zircon data from the Condrey Mountain schist (CMS), a unit of unknown origin exposed within a structural window in the central Klamath Mountains Province, as it provides key constraints on the Middle Jurassic to Early Cretaceous tectonic evolution of the Klamath Mountains Province. With new time constraints in hand, we reassess the mechanisms driving orogenesis, the formation of ophiolite-floored basins, and magmatism in the Klamath Mountains Province in the context of rapid changes in slab dip. These new data greatly facilitate regional correlation of the CMS, a longstanding regional geologic problem.

2. GEOLOGIC BACKGROUND

2.1. Paleozoic and Mesozoic Assembly of the Klamath Mountains Province

Numerous long (hundreds to thousands of kilometers), parallel, arcuate belts of accreted material comprise the North American Cordillera, which resulted from hundreds of millions of years of convergent margin tectonics following Neoproterozoic rifting of supercontinent Rodinia and the development of an "Atlantic-type" passive margin (Burchfiel et al., 1992; Dickinson, 2004; Blakey and Ranney, 2018). Here, we focus on Paleozoic and Mesozoic events germane to construction of the Klamath Mountains Province and adjacent Franciscan assemblages (Fig. 1).

Neoproterozoic to Devonian basement rocks of the Eastern Klamath terrane, interpreted as dismembered remnants of island arcs of the Paleo-Pacific (i.e., Panthalassa) Ocean, are the cornerstone of the Klamath Mountains upon which the remainder of the range was built (Moores, 1970; Speed, 1979; Burchfiel et al., 1992; Wallin and Metcalf, 1998; Wallin et al., 2000; Wright and Wyld, 2006; Grove et al., 2008; Fig. 1). Prior to docking with the western margin of North America in Silurian–Devonian time, oceanic assemblages of the Central Metamorphic terrane underplated the Eastern Klamath terrane along an east-dipping subduction zone (Davis, 1968; Irwin, 2003; Barrow and Metcalf, 2006). The resulting composite terrane was conveyed toward, and collided with, the western margin of North America via a west-dipping subduction zone, driving Late Permian–Early Triassic closure of the Golconda–Slide Mountain basin and eastward thrusting of deep-water assemblages atop shallow-water passive margin sequences in the Great Basin and adjacent areas (i.e., the Sonoma orogeny; Speed, 1977; Wyld, 1991; Burchfiel et al., 1992; Dickinson, 2000). Incorporation of the Eastern Klamath and Central Metamorphic terranes with the North American plate was accompanied by formation of the Fort Jones/Stuart Fork accretionary complex, the along-strike equivalent of the Cache Creek assemblage of the Canadian

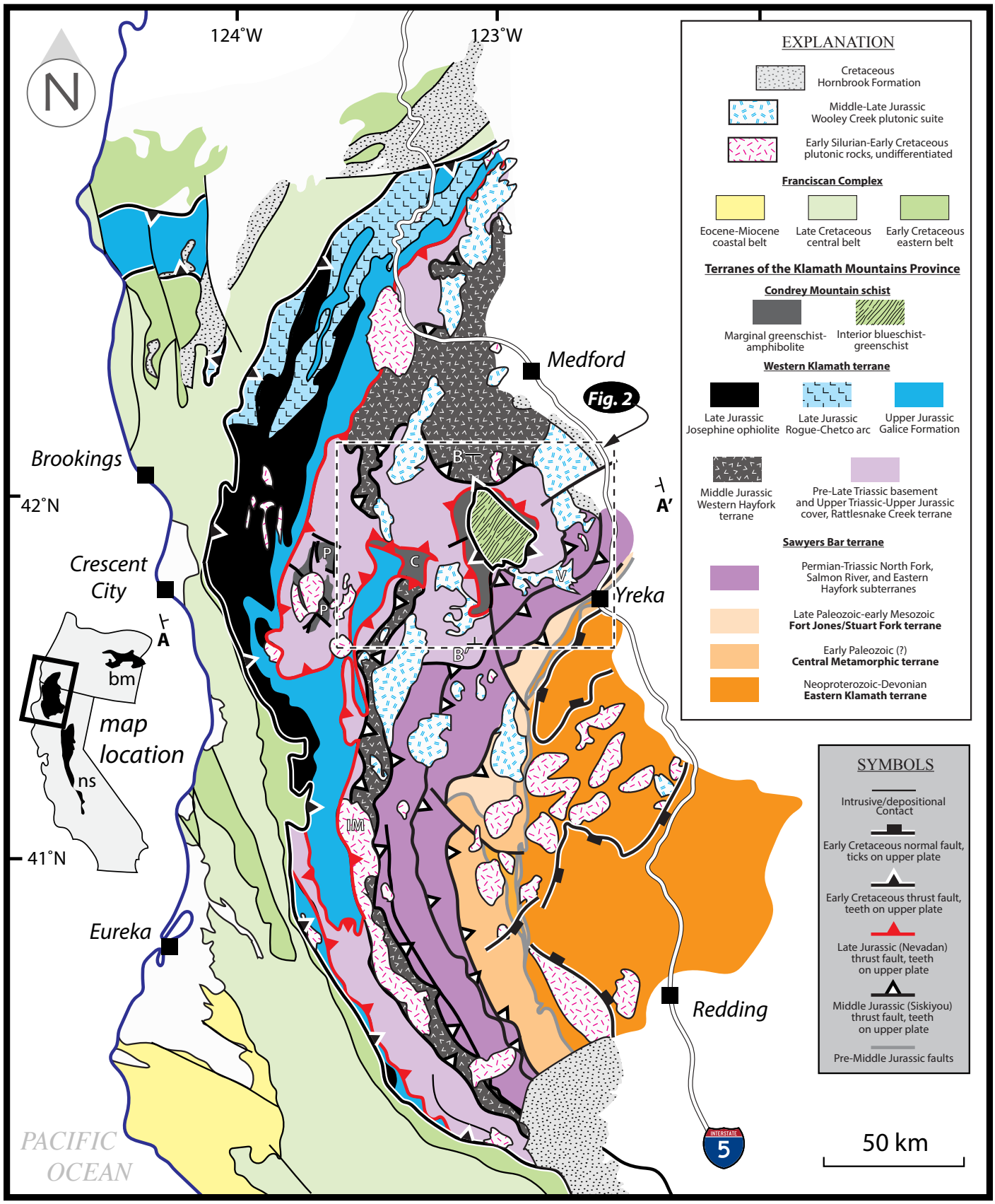

Figure 1. Simplified geologic and tectonic map of the Klamath Mountains Province, Northern California–southern Oregon, USA, modified after Blake et al. (1985) and Snoke and Barnes (2006). Traces of cross-sections A–A′ and B–B′ (Fig. 2) are overlain. Inset abbreviations: bm—Blue Mountains; ns—northern Sierra. Map abbreviations: C—China Peak Complex; P—Preston Peak Complex; IM—Ironside Mountain batholith; V—Vesa Bluffs pluton.

Cordillera (e.g., Johnston and Borel, 2007), and arc magmatism (the "McCloud arc" of Miller, 1987) above the eastward subducting lithosphere of Panthalassa (Wright, 1982; Coleman et al., 1988; Goodge, 1989).

The Paleozoic–early Mesozoic nucleus of the Klamath Mountains (i.e., the three terranes discussed in the previous paragraph) grew significantly during the Middle Jurassic (ca. 170 Ma) Siskiyou orogeny (Coleman et al., 1988; Wright and Fahan, 1988; Hacker et al., 1995; Snoke and Barnes, 2006; Barnes et al., 2006). This event involved sequential accretion of three additional "terranes." The first and most easterly is the Sawyers Bar terrane, formerly divided into the North Fork, Salmon River, and Eastern Hayfork subterranes, which together represent a Permian oceanic arc, overlying Permian–Triassic deep-sea and terrigenous sedimentary cover, plus outboard accretionary wedge (Coleman et al., 1988; Ernst, 1990; Hacker and Ernst, 1993, 1995; Scherer and Ernst, 2008; Scherer et al., 2010; Ernst et al., 2017). Accretion of the Western Hayfork terrane, a ca. 177–167 Ma continent-fringing oceanic arc (Harper and Wright, 1984; Wright and Fahan, 1988; Barnes and Barnes, 2020), and its dismembered ophiolitic basement—the Rattlesnake Creek terrane—followed (Wright and Fahan, 1988; Donato et al., 1996). The Rattlesnake Creek terrane consists of basal serpentinite matrix mélange, overlying ca. 193–207 Ma mafic volcanic plus and plutonic assemblages, and volcaniclastic and hemipelagic cover strata that are locally overprinted by amphibolite–granulite-facies parageneses (Irwin, 1972; Wright, 1982; Coleman et al., 1988; Wright and Wyld, 1994; LaMaskin et al., 2021).

The Rattlesnake Creek terrane is nonconformably overlain by pre-164 Ma greenschist-facies mafic intrusive and volcanic rocks plus hemipelagic sedimentary rocks (the Preston Peak Complex; e.g., Snoke, 1977; Saleeby et al., 1982) and tectonically underlain by ca. 172–170 Ma amphibolite-facies mafic volcanic rocks and hemipelagic sediments (the China Peak Complex; Saleeby and Harper, 1993). Both the China Peak and Preston Peak complexes are interpreted as early products of extension that culminated in the ca. 164–162 Ma Josephine ophiolite, the basement of the Western Klamath terrane (Saleeby and Harper, 1993). Lithologic and age similarities between the China Peak and Preston Peak complexes suggest that the former may represent the underthrust equivalent of the latter (Saleeby and Harper, 1993).

The Siskiyou event was immediately followed by rifting of newly accreted Rattlesnake Creek–Western Hayfork crust, forming the ca. 164–162 Ma Josephine ophiolite-floored basin. Rifting is envisioned to have occurred at a high-angle to the margin in a transtensional regime, such that the locus of spreading separated the active arc into the ca. 165–156 Ma Wooley Creek plutonic belt in the south and the ca. 161–155 Ma Rogue-Chetco arc in the north (Saleeby et al., 1982; Harper, 1984, 2003; Wright and Wyld, 1986; Wright and Fahan, 1988; Hacker and Ernst, 1993; Harper et al., 1994; Snoke and Barnes, 2006; Yule et al., 2006; Coint et al., 2013). For this reason, the Josephine basin has been deemed a site of ancient "interarc" rifting. This is misleading, however, as an interarc rift conjures images of parallel arcs separated by a rift. More accurately, rifting likely occurred in the forearc outboard of the Wooley Creek plutonic belt in the south (e.g., Harper, 2003), traversed the arc, and occurred in the retroarc inboard of the Rogue-Chetco arc in the north.

Deposition of the Galice Formation ensued in the submarine Josephine marginal basin, first with ca. 162–157 Ma (Oxfordian) argillite and transitioning to ca. 160–150 Ma (Oxfordian–Kimmeridgian) turbidite, as regional extensional stresses yielded to contractile deformation associated with the ca. 157–150 Ma Nevadan orogeny (Saleeby and Harper, 1993; Harper et al., 1994; Schweickert et al., 1984; Hacker et al., 1995; Miller and Saleeby, 1995; Shervais et al., 2004; MacDonald et al., 2006; Gradstein et al., 2020; LaMaskin et al., 2021; Surpless et al., 2024). The Nevadan event is responsible for thrusting the Western Klamath terrane (including the Rogue-Chetco arc plus consanguineous Josephine ophiolite and nonconformably overlying Galice formation) beneath previously accreted materials. There is no consensus at this time regarding the driving mechanism(s) for Nevadan and Siskiyou events. End-member models invoke either collisions of oceanic ridges or far-traveled lithospheric blocks such as the Wrangellia-Alexander superterrane (e.g., Schweickert and Cowan, 1975; Wernicke and Klepacki, 1988; McClelland et al., 1992; Saleeby and Harper, 1993; Shervais et al., 2004; Surpless et al., 2024), and/or changes in relative plate motion (e.g., Wright and Fahan, 1988; Wolf and Saleeby, 1995; Hacker et al., 1995; LaMaskin et al., 2021).

In Early Cretaceous time, the Klamath Mountains Province relocated ~200 km westward to achieve its current forearc position and concave-east arcuate curvature relative to correlative rocks in the northern Sierra Nevada and Blue Mountains (Fig. 1 inset; Jones and Irwin, 1971; Ernst, 2013). Following this episode, (1) magmatism in the Klamaths abruptly terminated at ca. 136 Ma, in marked contrast to the Sierra Nevada and Blue Mountains, where magmatism continued until Late Cretaceous time (Chen and Moore, 1982; Lund and Snee, 1988; Barnes et al., 1996; Allen and Barnes, 2006); (2) an accretionary wedge, represented by the eastern belt of the Franciscan Complex, formed and grew rapidly along the western edge of the Western Klamath terrane (Dumitru et al., 2010); (3) the Western Klamath terrane, eastern belt Franciscan rocks, and the Condrey Mountain schist (discussed in the following section) cooled from ~400 °C to ~200 °C between ca. 135 Ma and 118 Ma (Helper, 1985; Harper et al., 1994; Batt et al., 2010a; Dumitru et al., 2010; Tewksbury-Christle et al., 2021); (4) low-angle normal faulting commenced in the eastern Klamath Mountains (Cashman and Elder, 2002; Batt et al., 2010b); and (5) topography built up during earlier tectonism was lost during an eastward-sweeping Valanginian–Hauterivian marine transgression across the majority of the Klamath Mountains Province (Harper et al., 1994; Batt et al., 2010a). The significance of these relations and a discussion of possible driving mechanisms are explored in section 5.4.

2.2. Condrey Mountain Schist

The CMS stands out as an unusual feature of the Klamath Mountains Province. The unit is exposed as a domal structural window through the overlying Rattlesnake Creek terrane, beneath the low-angle Condrey Mountain shear zone (Mortimer and Coleman, 1985; Fig. 2). This structural arrangement

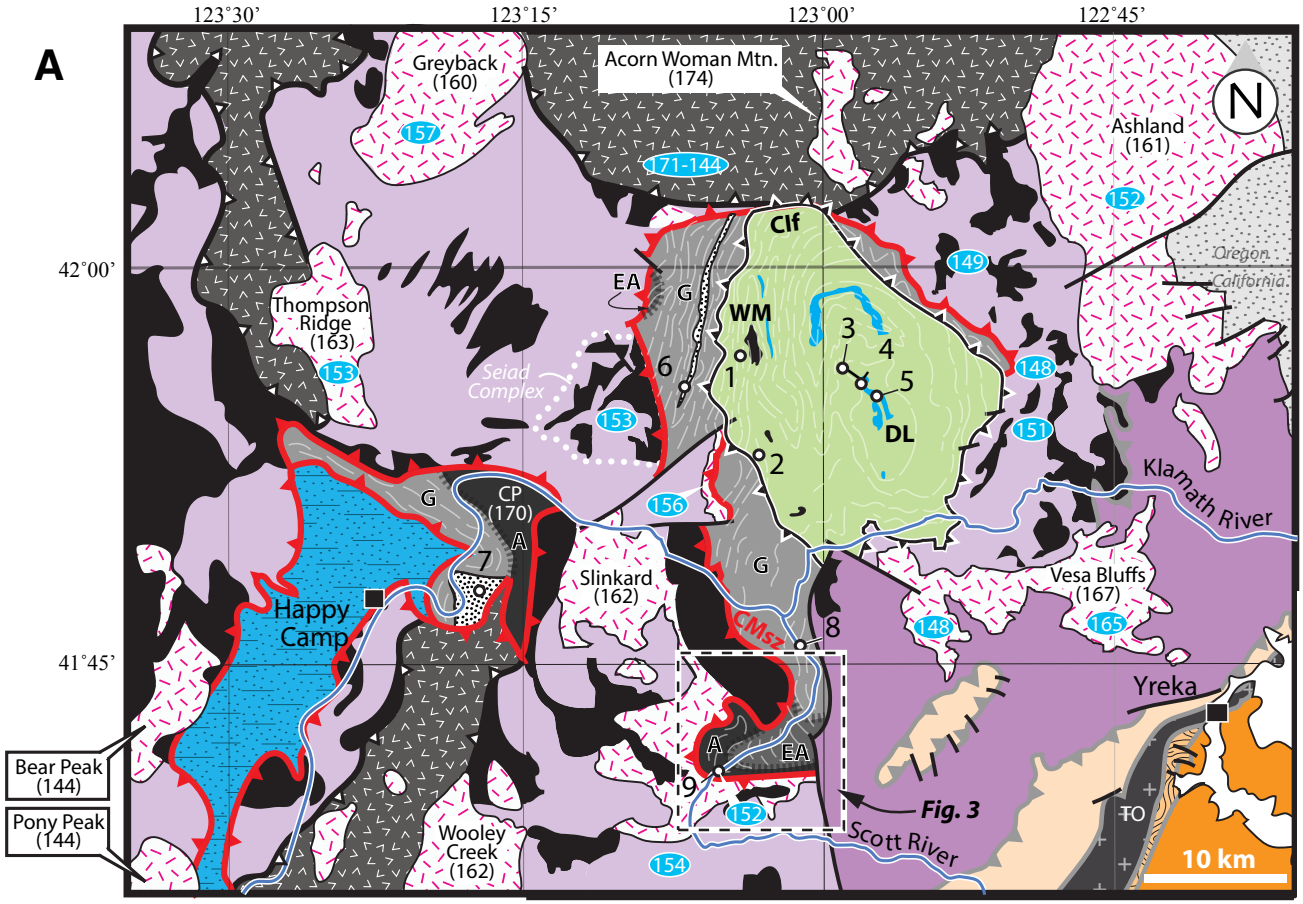

EXPLANATION

Cretaceous Hornbrook Formation

Mesozoic plutonic rocks (U-Pb zircon age [Ma] in parentheses)

Terranes of the Klamath Mountains Province

Condrey Mountain schist (CMS)

Semipelite — Marginal unit

Serpentinite — Inner unit

Coherent blueschist

Terrane 6 (Western Klamath terrane)

Upper Jurassic Galice Formation

Terrane 5

Ultramafic rocks

A: Middle Jurassic Western Hayfork terrane

B: Pre-Late Triassic basement and Upper Triassic-Upper Jurassic cover, Rattlesnake Creek terrane

Terrane 4 (Sawyers Bar terrane)

Permian-Triassic North Fork, Salmon River, and Eastern Hayfork subterranes

Terrane 3 — Late Paleozoic-early Mesozoic Fort Jones/Stuart Fork terrane

Terrane 2 — Early Paleozoic (?) Central Metamorphic terrane

Terrane 1 — Neoproterozoic-Devonian Eastern Klamath terrane

SYMBOLS

Early Cretaceous thrust fault, teeth on upper plate

Intrusive or depositional Contact

151 Amphibole $^{40}Ar/^{39}Ar$ cooling age

Late Jurassic (Nevadan) thrust fault, teeth on upper plate

Gradational Contact

7 Location of sample listed in Table 1

Late Cretaceous and younger faults

G/EA/A Metamorphic grade of outer CMS and equivalents (G, greenschist; EA, epidote amphibolite; A, amphibolite)

Middle Jurassic (Siskiyou) thrust fault, teeth on upper plate

Pre-Middle Jurassic thrust faults, teeth on upper plate

Figure 2. (A) Simplified geologic map of the central Klamath Mountains Province, Northern California–southern Oregon, USA, modified after Hotz (1979), Barrows (1969), Hill (1984), Burton (1982), Helper (1986), and Saleeby and Harper (1993). Note that many faults identified with thrust symbols have been variably reactivated in a normal sense. Amphibole $^{40}Ar/^{39}Ar$ ages are from Saleeby and Harper (1993), Hacker and Ernst (1993), Hacker et al. (1995), and Donato et al. (1996). Zircon U-Pb ages are from Snoke and Barnes (2006). See Figure 1 for map location. Sampled locations (white-filled circles) are overlain; sample numbers correspond to those in Table 1. Abbreviations: CP—China Peak; DL—Dry Lake; TO—Trinity ophiolite; WM—White Mountain; CMsz—Condrey Mountain shear zone. (*Continued on following page.*)

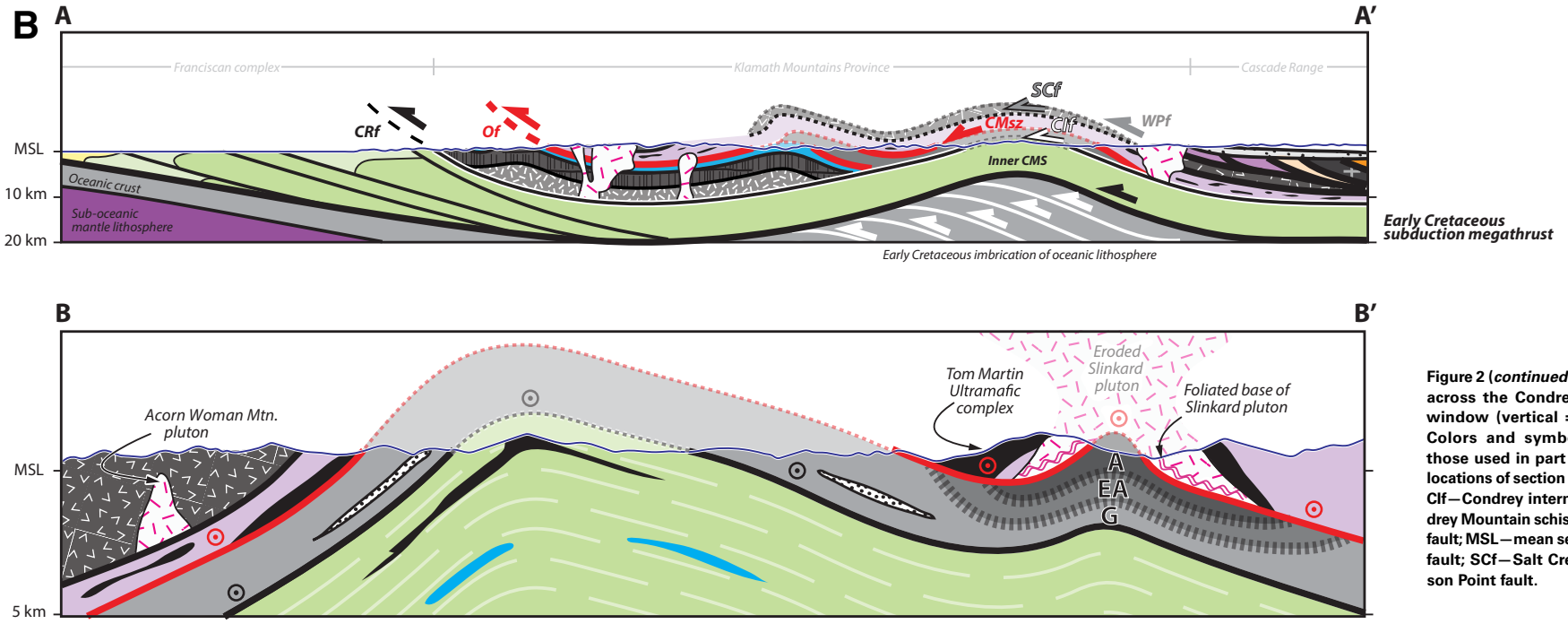

Figure 2 (*continued*). (B) Cross-sections across the Condrey Mountain schist window (vertical = horizontal scale). Colors and symbols correspond to those used in part A. See Figure 1 for locations of section lines. Abbreviations: Clf—Condrey internal fault; CMS—Condrey Mountain schist; CRf—Coast Range fault; MSL—mean sea-level; Of—Orleans fault; SCf—Salt Creek fault; WPf—Wilson Point fault.

significantly differs from the usual westward-younging stack of east-dipping thrust sheets observed in the Klamath Mountains Province. Furthermore, the CMS resides at lower metamorphic grade and yields younger cooling ages relative to flanking rocks (Helper, 1985; Hacker et al., 1995; Tewksbury-Christle et al., 2021). Efforts to fit the CMS into the regional puzzle have focused on lithologic and age similarities with adjacent rocks, resulting in correlations with the Central Metamorphic terrane (Irwin, 1960), Stuart Fork terrane (Medaris, 1966), the Galice Formation (Klein, 1977; Hotz, 1979; Saleeby and Harper, 1993), the China Peak Complex (Saleeby and Harper, 1993), and the South Fork Mountain schist (the oldest Franciscan unit of significant areal size; Suppe and Armstrong, 1972; Brown and Blake, 1987). The Central Metamorphic and Stuart fork terranes are now known to be significantly older than the CMS, which renders earlier correlations untenable (Hotz et al., 1977).

The CMS is subdivided into a structurally deeper, relatively low-grade inner unit and a structurally higher, relatively high-grade marginal unit, which are separated by the Condrey internal fault (Helper, 1986; Saleeby and Harper, 1993; Figs. 1 and 2). Both CMS subunits preserve similar prograde, ductile, non-coaxial deformation and texturally late coaxial flattening fabrics, which are attributed to subduction-related burial and later structural ascent, respectively (Helper, 1986).

The inner CMS consists chiefly of greenschist–blueschist-grade graphitic and quartz-mica schist, which was likely produced through metamorphism of argillite and chert protoliths, which locally contain lenses and tabular slabs of blueschist (formerly basaltic flows and tuff) and serpentinite (Hotz, 1979; Helper, 1986; Saleeby and Harper, 1993; Tewksbury-Christle et al., 2021). The array of rock types observed within the inner CMS, and the paucity of clastic material therein, point to sedimentation in an open ocean starved of terrigenous input atop a basement and/or including olistoliths of oceanic lithosphere.

The outer CMS mantles the inner unit and includes greenschist–amphibolite-facies metamorphosed basaltic tuffs, pillow lavas, and rare comagmatic intrusive equivalents and plagiogranite. These igneous protoliths dominate the outer CMS, though they are locally interrupted by lenses of hemipelagic material (now silicic and graphitic quartz-mica schist) and one prominent (~10-km-long × 0.5-km-wide in map view) semi-pelitic horizon exhibiting graded beds, which likely represents deep-water turbidite deposits (Hotz, 1979; Helper, 1985). The range of lithologies observed in the outer CMS suggests oceanic deposition proximal to an eruptive center with sporadic input of terrigenous material.

Along the "Scott River appendage," the outer CMS reaches amphibolite facies as the Condrey Mountain shear zone is approached from below (Saleeby and Harper, 1993; Figs. 2 and 3). Metamorphic grade also increases

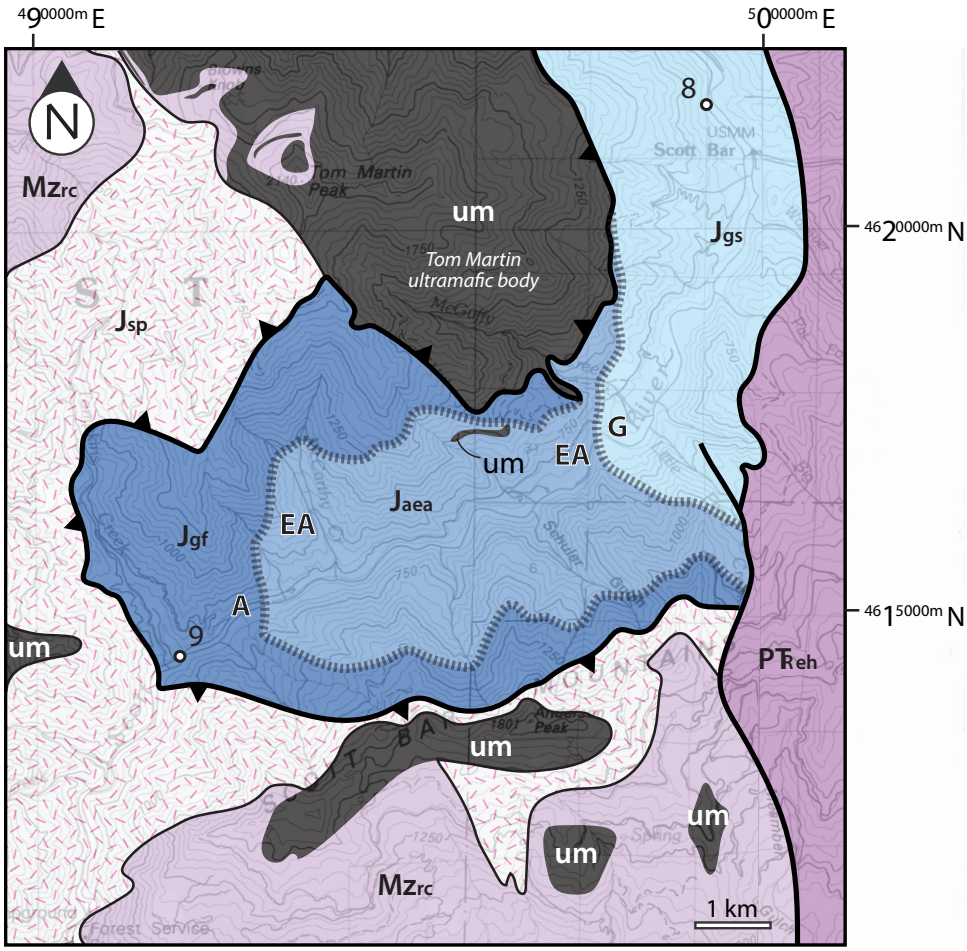

Figure 3. Simplified geologic map of the Scott River appendage, modified after Hotz (1979), Barrows (1969), Cornwall (1981), Burton (1982), and Saleeby and Harper (1993). Map base: U.S. Geological Survey (1979, 1983) 30 × 60 min series (1:100,000 scale) maps of Yreka and Happy Camp quadrangles (The National Geologic Map Database, https://ngmdb.usgs.gov). Sampled localities are overlain. See Figure 2A for map location. CMSf—Condrey Mountain schist.

down-section within the Rattlesnake Creek terrane, preserving upper amphibolite- and locally granulite-facies parageneses, as the Condrey Mountain shear zone is approached from above (Hotz, 1979; Mortimer and Coleman, 1985; Garlick et al., 2009). These relations require a sharp, inverted metamorphic field gradient spanning structurally deep, low-grade inner CMS and higher grade outer CMS.

3. METHODS

3.1. U-Pb Geochronology

Ten samples were collected for U-Pb zircon analysis: (1) three samples from the outer CMS (two from a plagiogranite inclusion transposed into the main foliation of surrounding actinolite schist previously investigated by Saleeby and Harper [1993], and one from the semi-pelite of Helper [1985]); (2) five samples from the inner unit (three from the "Dry Lake" area of Helper [1985], the deepest exposed level of the CMS, and two from structurally higher); (3) one sample from the Gold Flat amphibolite (Burton, 1982) of uncertain affinity (either representing the base of the Rattlesnake Creek terrane or the top of the outer CMS); and (4) one sample of uncertain origin from a structurally complex zone ~5 km east of Happy Camp, California (representing hemipelagic protoliths of either the Galice formation or CMS). Table 1 provides coordinates for all localities sampled.

Zircon grains were extracted using standard mineral separation techniques: crushing, sieving, magnetic separation, processing through heavy liquids, and hand picking. Separates were then mounted in epoxy, polished, and imaged on the Macalester Keck Lab JEOL 6610LV scanning electron microscope (SEM) before analysis.

U-Pb geochronology of igneous and detrital zircon was conducted by laser ablation–multicollector–inductively coupled plasma–mass spectrometry (LA-MC-ICP-MS) at the Arizona LaserChron Center (ALC) following the methods outlined in Gehrels et al. (2006). Zircon grains were ablated using a 193 nm ArF laser with a pit depth of ~12 µm and spot diameters of 35 µm for sample 14CM21 and 20 µm for all other samples. Fragments of in-house Sri Lanka (SL) and Forest Center (Duluth Complex; FC-1) zircon standards, with isotope dilution–thermal ionization mass spectrometry (ID-TIMS) ages of 563.5 ± 3.2 Ma and 1099 ± 0.6 Ma (2σ), respectively, were analyzed once per every five unknown analyses to correct for instrument mass fractionation (Paces and Miller, 1993; Gehrels et al., 2008). A secondary standard, R33 (Black et al., 2004), with an ID-TIMS age of 418.9 ± 0.4 Ma (2σ), was analyzed once per every 50 unknown analyses. A weighted mean $^{206}Pb/^{238}U$ age of 420.4 ± 3.5 Ma (2σ, mean square of weighted deviates [MSWD] = 0.22) was calculated from a total of 29 analyses of R33 performed at the ALC. Data reduction was done using in-house ALC Microsoft Excel programs and Isoplot/Ex Version 3 (Ludwig, 2003). This process included calculation of average intensity, correction for background interference, and calculation of isotopic ratios and ages. Analyses with >10% uncertainty, 20% discordance, and/or 5% reverse discordance were excluded. Normalized, cumulative probability and multidimensional scaling plots were constructed with detritalPy (Sharman et al., 2018) using $^{207}Pb/^{206}Pb$ ages for grains older than 900 Ma and $^{206}Pb/^{238}U$ ages for grains younger than 900 Ma.

Detrital geochronology provides constraints on the maximum depositional ages (MDAs) of (meta)sedimentary rocks, though a wide range of techniques exists for calculating MDAs (e.g., Dickinson and Gehrels, 2009; Sharman et al., 2018; Coutts et al., 2019; Vermeesch, 2021). Methods based on the youngest single grain (YSG), the youngest clusters of grains, and Tuff-Zirc or AgePick algorithms were avoided as they drift to younger ages as the number of analyses increases (Vermeesch, 2021). Similarly, estimates based on the weighted mean or mode of the youngest peak of a probability density plot were not used due to underlying issues of probability density plots (Vermeesch, 2012). We present MDAs in Table 2 calculated via the youngest statistical population (YSP; Coutts et al., 2019) and maximum likelihood algorithm (MLA; Vermeesch, 2021) techniques, as these methods are least likely to yield ages younger than the true depositional age. The "interpreted age" column in Table 2 factors in MDA calculations and regional thermochronologic data, if available.

TABLE 1. SAMPLE LOCATIONS AND DESCRIPTIONS

Sample	Abbreviation	Rock unit	Description	UTM Zone	UTM Easting	UTM Northing
15KM14	1	WM CMS	Graphitic schist	10T	494664	4644493
15KM11	2	WM CMS	Graphitic schist	10T	495747	4637173
14CM16	3	Inner CMS	Graphitic schist	10T	501716	4642816
19KM5	4	Inner CMS	Graphitic schist	10T	503222	4641838
19KM4	5	Inner CMS	Graphitic schist	10T	503868	4641015
15KM23	6	Outer CMS	Semipelite of Helper (1985)	10T	490621	4642545
19KM3	7	Unknown; Outer CMS	Quartzofeldspathic schist	10T	476118	4627262
15KM49/14CM1	8	Outer CMS	Metamorphosed felsic stock	10T	499148	4621960
14CM21	9	Unknown; Outer CMS	Gold Flat amphibolite of Burton (1982)	10T	491966	4614462

Notes: WM—White Mountain; CMS—Condrey Mountain schist; UTM—Universal Transverse Mercator.

TABLE 2. DEPOSITIONAL AGE CONSTRAINTS FOR DETRITAL ROCKS STUDIED

Sample	Abbreviation	Rock unit	N	YSG (Ma)	YSG 2σ (Ma)	YSP*	2σ	MSWD	MLA* (Ma)	2σ	Most relevant deposition-bracketing age (Ma)	Interpreted depositional age
15KM23	6	Outer CMS	135	161.6	8.4	169.5	1.9	1.0	170.8	2.0	156–152[†]	Middle or Upper Jurassic
15KM14	1	WM CMS	90	156.5	7.9	159.8	3.5	0.6	159.8	3.5	144[§]	Upper Jurassic
15KM11	2	WM CMS	119	141.1	5.1	144.5	3.2	1.2	153.4	2.6	144[§]	Upper Jurassic or Lower Cretaceous
14CM16	3	Inner CMS	73	131.7	7.8	139.5	4.0	1.7	142.5	5.0	128[#]	Lower Cretaceous
19KM5	4	Inner CMS	274	129.5	8.5	135.1	2.1	1.0	135.5	2.3	128[#]	Lower Cretaceous
19KM4	5	Inner CMS	283	128.9	2.9	130.7	2.1	1.6	130.2	3.5	128[#]	Lower Cretaceous
19KM3	7	Unknown	184	151.4	16.2	162.1	1.6	1.0	164.2	1.6	Not available	Upper Jurassic

Notes: See text for discussion of maximum depositional age calculations. MSWD—mean square of weighted deviates; N—number of grains analyzed; YSG—youngest single grain; YSP—youngest statistical population (Coutts et al., 2019); MLA—maximum likelihood algorithm (Vermeesch, 2021); WM—White Mountain; CMS—Condrey Mountain schist.
*YSP (Coutts et al., 2019) and MLA (Vermeesch, 2021) uncertainties include both analytical and systematic uncertainties.
[†]K-Ar and Ar-Ar hornblende (Helper, 1985; Saleeby and Harper, 1993)
[§]K-Ar white mica (Lanphere et al., 1968)
[#]K-Ar white mica (Helper, 1985)

4. RESULTS

4.1. Petrography and Metamorphic Petrology

Samples 14CM16, 15KM11, 15KM14, 19KM4, and 19KM5 were all collected from the internal metasedimentary CMS unit. Of these, samples 14CM16, 19KM4, and 19KM5 are from the Dry Lake area of Helper (1986), the deepest exposed portion of the CMS. At this location, these hemipelagic protoliths are recumbently folded with metamorphosed mafic volcanic assemblages that equilibrated at pressure-temperature (*P-T*) conditions of 380–450 °C and 6–11 kbar (Helper, 1986; Tewksbury-Christle et al., 2021; Fig. 4A). Additional constraints are placed on the *P-T* trajectory of metamorphism in the CMS through thermodynamic modeling. The Gibbs free-energy minimization software package Theriak-Domino (de Capitani and Brown, 1987) and the thermodynamic end-member and solution models of the accompanying tc321p2 database (Thermocalc database as distributed in version 3.33) were used to construct *P-T* pseudosections in the NCKFMASH system.

Dry Lake metasedimentary rocks contain chiefly medium- to fine-grained quartz, albitic plagioclase, phengitic to paragonitic white mica, carbonaceous material, and chlorite, which locally exhibits pseudomorphs after pyrite of up to 1 cm in diameter. Minor phases include epidote, zoisite, titanite, and stilpnomelane. Thermodynamic modeling, using bulk compositions reported by Hotz (1979), shows this mineral paragenesis to be stable at the conditions reported above for metavolcanic units, which corroborates the assertion that metavolcanic and metasedimentary assemblages at Dry Lake represent metamorphosed relict stratigraphy (Helper, 1986; Fig. 5). These samples exhibit well-developed flattening fabrics containing tight to isoclinal and disharmonic folds that are best expressed by intervals rich in white mica and carbonaceous material (Fig. 4B).

Samples 15KM14 and 15KM11 were collected from the structural top of the inner CMS in the vicinity of White Mountain, <1 km from the Condrey internal fault, and exhibit mylonitic foliation characterized by spaced white (quartz plus albite) and pale- to medium-green (chlorite, white mica, and carbonaceous material) domains with local preservation of tight isoclinal folds (Fig. 4C). Pyrite pseudomorphs similar to those at the Dry Lake area were observed in the outcrop from which sample 15KM14 was extracted. Notably, these samples lack epidote group minerals, which suggests that peak metamorphic temperatures in the vicinity of White Mountain were ~100 °C higher, at similar pressure, than those achieved in the Dry Lake area (Fig. 5).

The bulk of the outer CMS consists of albitic plagioclase, actinolite, chlorite, epidote, and white mica with minor quartz and titanite, which is consistent with equilibration of these metavolcanic assemblages under greenschist-facies conditions (Fig. 5). Sample 15KM23 is from a semi-pelitic interval in the otherwise metabasaltic marginal unit of the CMS (Fig. 2; Helper, 1985, 1986). This sample exhibits alternating, highly cleaved chlorite- and carbonaceous-rich domains and microlithons containing subequal proportions of quartz and chlorite (Fig. 4D). Plagioclase is apparently lacking from this sample, and epidote is observed as a minor phase throughout the sample and appears to have statically overgrown cleaved and microlithon domains that formed earlier.

Sample 14CM21, collected from the Gold Flat amphibolite of either the uppermost CMS or lowermost Rattlesnake Creek terrane, is a coarse blastomylonitic amphibolite gneiss containing chiefly pargasitic amphibole, anorthitic plagioclase, and epidote, with minor apatite and ilmenite, and rare coarse (~1 cm) garnet porphyroblasts (Figs. 4E and 4F). The Gold Flat amphibolite equilibrated at peak metamorphic conditions of 630 ± 50 °C at 7.3 ± 1.0 kbar, which correspond to transitional albite–epidote amphibolite/upper amphibolite-facies conditions (Klapper and Chapman, 2017) and overlap the H_2O-saturated solidus for outer CMS metabasite (Fig. 5).

Samples 14CM17 and 15KM49 were collected from a coarse-grained felsic interval displaying a foliation concordant with that of encasing outer CMS actinolite schist. These relations point to an intrusive protolith that invaded

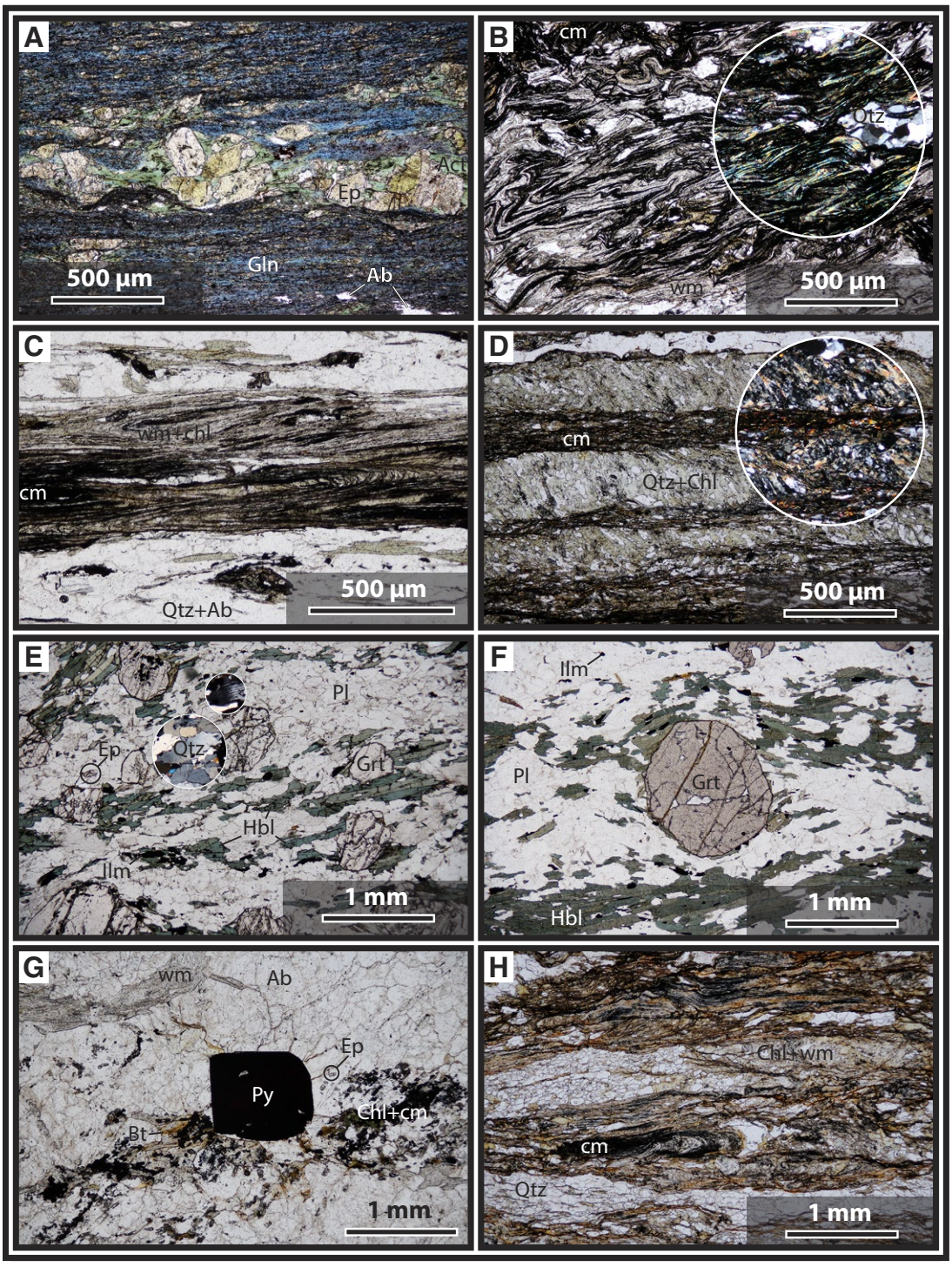

Figure 4. Thin-section photomicrographs of petrologic and structural features in the Condrey Mountain Schist, central Klamath Mountains Province, and adjacent lithologies. (A) Transitional blueschist–greenschist-facies metabasalt from the Dry Creek subunit in plane-polarized light. (B) Disharmonic folds in Dry Lake metasedimentary rocks in plane-polarized light. Circular "spotlight" inset is shown in cross-polarized light. (C) Intrafolial isoclinal folds in metasedimentary rocks from the White Mountain subunit in plane-polarized light. (D) Highly cleaved (dark) and microlithon (light green) domains in semipelitic rocks of the outer Condrey Mountain Schist in plane-polarized light. Spotlight is shown in cross-polarized light. (E) Garnet-bearing Gold Flat amphibolite in plane-polarized light. Note tapered deformation twins in plagioclase plus amoeboid grain boundaries in undulose quartz (both shown in cross-polarized light spotlights), which suggests deformation at elevated shear stress and temperature. (F) Large garnet porphyroblast in Gold Flat amphibolite in plane-polarized light (note that garnet in this unit locally achieves diameters of ~1 cm). (G) Leucogneiss of the outer Condrey Mountain Schist exposed north of Scott Bar showing plagioclase- and mica-dominated assemblage. Chlorite pseudomorph after pyrite at center, in plane-polarized light. (H) Metasedimentary assemblages of uncertain origin exposed along Klamath River assemblage, in plane-polarized light. Note ruptured isoclinal fold adjacent to "cm" annotation. Mineral abbreviations: Ab—albite; Act—actinolite; Bt—biotite; cm—carbonaceous material; Chl—chlorite; Ep—epidote; Gln—sodic amphibole (glaucophane/crossite); Grt—garnet; Hbl—hornblende; Ilm—ilmenite; Pl—plagioclase; Py—pyrite; Qtz—quartz; wm—white (phengitic) mica.

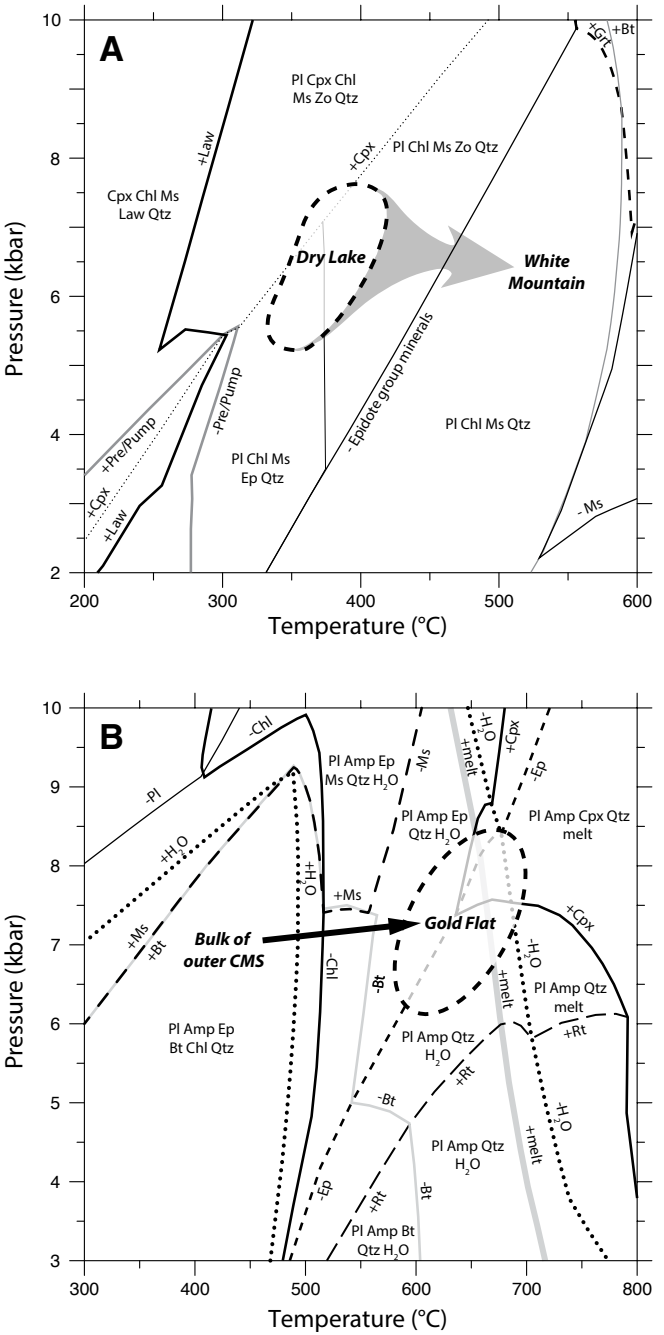

Figure 5. Calculated pressure-temperature (*P-T*) pseudosections for (A) inner and (B) outer Condrey Mountain schist (CMS) compositions. Dry Creek *P-T* estimate of Helper (1986) is overlain in part A. Gold Flat *P-T* estimate of Klapper and Chapman (2017) is overlain in part B. Modeled bulk compositions are from Hotz (1979).

the outer CMS prior to underthrusting and metamorphism. These samples are dominated by quartz and albitic plagioclase with subsidiary white mica, biotite, chlorite, and pyrite (Fig. 4G).

The NE margin of a reentrant of Western Klamath terrane assemblages paralleling the Klamath River (the "Klamath River Appendage" of Saleeby and Harper, 1993) is of uncertain affinity. While most maps assign exposed greenschist-facies hemipelagic rocks to the Galice Formation, Hill (1984) interprets these rocks as a <5-km-wide window of inner CMS lying structurally above the Galice Formation and beneath the China Peak Complex. Sample 19KM3 was collected from this window with the aim of clarifying the affinity of these rocks (Fig. 2). This sample contains a greenschist-facies assemblage of quartz, chlorite, white mica, carbonaceous material, and minor epidote, arranged in tightly folded quartz-rich and micaceous domains (Fig. 4H).

4.2. Zircon U-Pb Geochronology

Results from U-Pb zircon analysis of the CMS and samples of unknown affinity are reported below, summarized in Table S1 in the Supplemental Material,[1] and illustrated in Figures 6 and 7.

4.2.1. CMS Igneous Analysis

15KM49 and 14CM17. These samples of meta-plagiogranite yielded 46 and 107 concordant U-Pb zircon ages, respectively, from which a concordia age of 171.8 ± 0.8 (2σ) was calculated (Fig. 6). This age is identical within uncertainty to a 172 ± 2 Ma age reported by Saleeby and Harper (1993) from an ~100-m-scale gneissic metadiorite sill collected <5 km from the locality studied.

4.2.2. CMS Detrital Analyses

15KM23. This sample is from the western portion of the marginal CMS unit and is the structurally highest metasedimentary sample studied here. Concordant ages from 135 zircon grains range from 161.4 ± 4.8 Ma to 2898.3 ± 12.0 Ma (1σ; Fig. 7). The sample yields YSP and MLA MDAs of 169.5 ± 0.6 Ma

[1]Supplemental Material. U-Pb zircon data from the Condrey Mountain schist and adjacent units. Please visit https://doi.org/10.1130/GEOS.S.25316140 to access the supplemental material, and contact editing@geosociety.org with any questions.

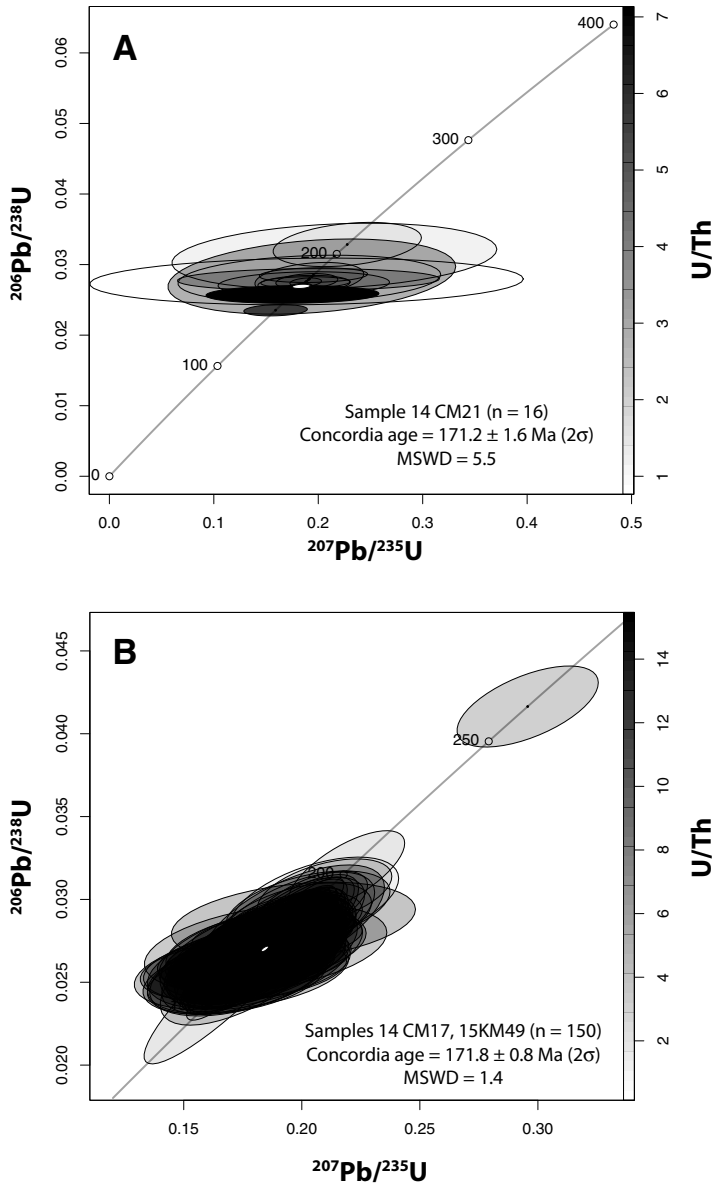

Figure 6. U-Pb zircon concordia plots (from laser ablation–inductively coupled plasma–mass spectrometry analysis) from (A) Gold Flat amphibolite melanosomes, and (B) leucogneiss collected from ~0.4 miles north of Scott Bar (Fig. 3). Individual analyses are shown as unfilled black ellipses; calculated concordia ages are shown as white ellipses with black fill. MSWD—mean square of weighted deviates.

and 170.8 ± 0.7 Ma (1σ), respectively. Notably, these values are based on a large cluster of ~50 ages that overlap at the 1σ level and are probably too conservative. The majority of grains analyzed (54%) yield Jurassic ages, with the most pronounced peak centered at 168 Ma. Paleozoic populations (21% of the total) exhibit minor peaks at 268 Ma, 320 Ma, 329 Ma, 390 Ma, and 486 Ma. "Timanian/Pan-African-age" (i.e., 540–700 Ma) grains make up 5% of the total. Proterozoic populations include a broad swath of "Grenville-age" (i.e., 950–1300 Ma) grains (7%) plus distinct peaks at 1350 Ma, 1500 Ma, and 1630 Ma, which correspond to 5%, 3%, and 5% of grains analyzed, respectively. Four isolated Archean grains range from 2500 Ma to 2900 Ma.

15KM14. MDAs of 159.8 ± 1.6 Ma (1σ) were calculated from this sample (YSP and MLA methods produce identical results), which yielded 90 concordant U-Pb zircon ages ranging from 156.5 ± 3.9 Ma to 2484.1 ± 24.9 Ma (1σ). This sample is characterized by a spiky distribution of U-Pb ages, with peaks at ca. 160 Ma, 410 Ma, 1020 Ma, 530 Ma, and 620 Ma. Jurassic, Paleozoic, Timanian/Pan-African, and Grenville age components comprise 10%, 30%, 11%, and 24% of the total, respectively. Scattered Proterozoic grains with ages of >1100 Ma plus one ca. 2750 Ma grain comprise 28% of the grains analyzed.

15KM11. This sample yielded 119 concordant U-Pb zircon ages suitable for provenance analysis and the largest disparity among MDAs calculated (YSP: 144.5 ± 1.5 Ma; MLA: 153.4 ± 1.1 Ma; 1σ). Grains analyzed range in age from 141.1 ± 2.5 Ma to 2958.2 ± 20 Ma (1σ). In this sample, 24.3% of the grains are Jurassic, exhibiting a distinct peak at ca. 158 Ma and an auxiliary peak at ca. 190 Ma. Paleozoic ages comprise 18% of the total and exhibit numerous minor age peaks at ca. 275 Ma, 325 Ma, and 365–440 Ma. A distinct population of Timanian/Pan-African ages (8%) with a peak at ca. 610 Ma, Grenville-age grains (16%), and less prominent peaks at ca. 1450 Ma, 1500 Ma, and 1680 Ma comprise the bulk of the remaining ages. This sample also yielded three ca. 2000 Ma and two 2900 Ma ages.

14CM16. This sample was collected from the summit of Condrey Mountain at the northern edge of the Dry Lake area (Helper, 1986), which is the deepest exposed portion of the Condrey Mountain structural window. The 73 concordant U-Pb zircon ages from this sample range from 131.7 ± 3.9 Ma to 2078.2 ± 44.3 Ma (1σ) and yield MDAs, calculated using the YSP and MLA methods, of 139.5 ± 1.9 Ma and 142.5 ± 2.4 Ma (1σ), respectively. As in other samples analyzed from the CMS, the largest peak in terms of area is Jurassic (22% of the total), with a peak falling at ca. 160 Ma. Auxiliary early Mesozoic age peaks are observed at ca. 225 Ma and 250 Ma. Paleozoic populations (15% of the total) are concentrated at ca. 340 Ma, 430 Ma, and 510 Ma. A population of Timanian/Pan-African ages comprises 16% of the grains analyzed and exhibits a conspicuous ca. 600 Ma peak. Grenville-age grains exhibit a peak at ca. 1030 Ma and account for 19% of the sample. Scattered Proterozoic ages with one low-relief peak at 1450 Ma comprise most of the remaining ages.

19KM5. This sample was collected 2 km SE of sample 14CM16, within the Dry Lake area, and yielded 274 U-Pb ages suitable for provenance analysis. These ages span 129.5 ± 4.3 Ma to 3295.4 ± 12.1 Ma (1σ) and yield YSP and MLA MDAs of 135.1 ± 0.9 Ma and 135.5 ± 1.0 Ma (1σ), respectively. In order

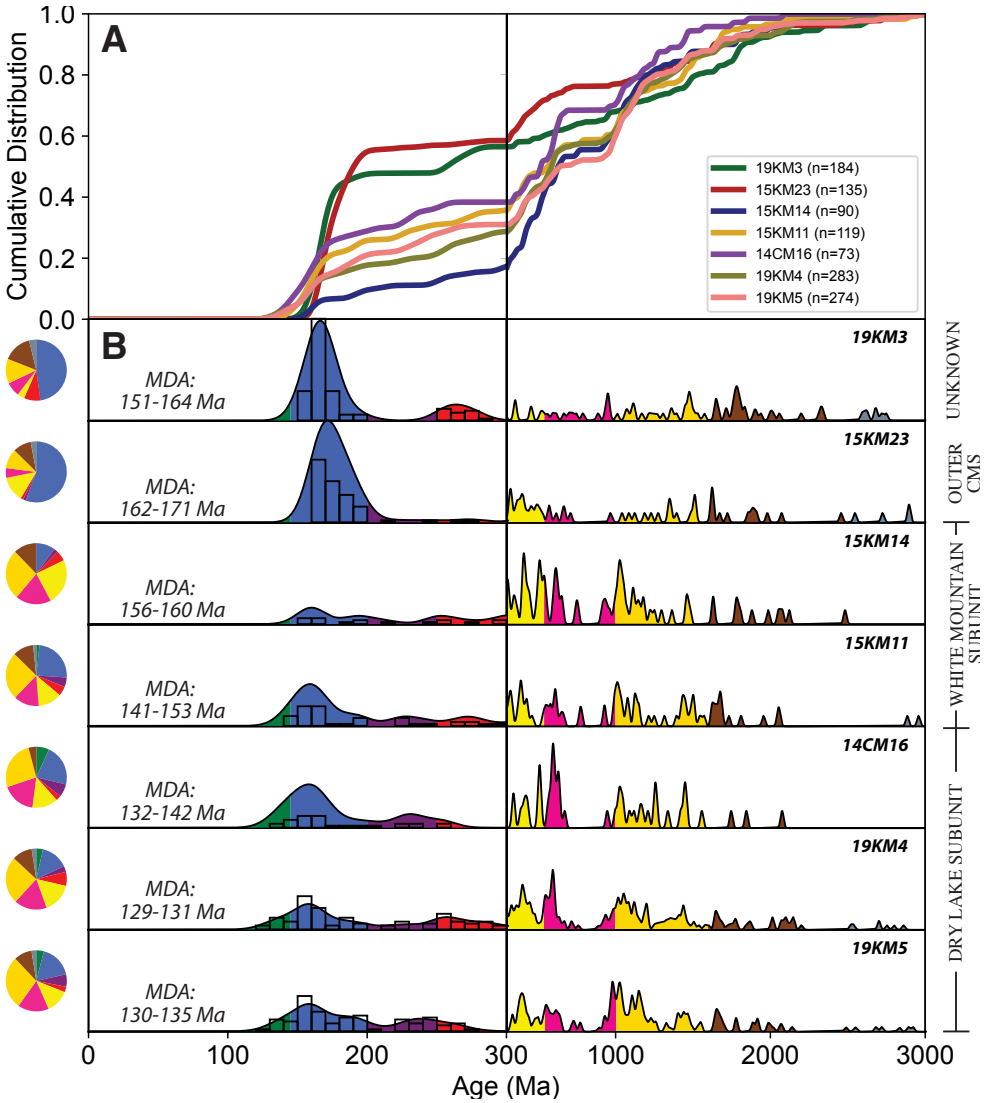

Figure 7. (A) Cumulative probability plot, and (B) corresponding normalized kernel density estimates (KDE) with 10 m.y. bandwidth comparing detrital zircon ages from samples collected from the Condrey Mountain schist (CMS). Note the split horizontal axis at 300 Ma and that spectra between 300 Ma and 3000 Ma are vertically exaggerated by a factor of five. Pie diagram bin colors correspond to those beneath each KDE curve. Maximum depositional age (MDA) ranges are provided in Table 2. Uncertainties are 2σ. n—number of concordant analyzed grains.

of decreasing prominence, the age peaks exhibited by this sample are at ca. 158 Ma (with a broad Jurassic shoulder comprising 18% of total grains), 240 Ma, Grenville-age grains (26%) with peaks at 1020 Ma and 1150 Ma, Paleozoic ages (15%) with a 390 Ma peak, and Timanian/Pan-African populations (7%) at ca. 550 Ma and 610 Ma. Pre-Grenville-age grains are generally scattered, with discernable peaks at ca. 1440 Ma, 1660 Ma, and 1910 Ma, and with an array of Neoarchean ages.

19KM4. This sample was collected 1 km SE of the previous sample, again from the Dry Lake area, and yielded 284 concordant U-Pb ages ranging from 128.2 ± 2.2 Ma to 2862.6 ± 10.3 Ma (1σ). Respectively, YSP and MLA MDAs of 130.7 ± 0.9 Ma and 130.2 ± 1.7 Ma (1σ) were calculated from this sample. Jurassic, Paleozoic, Timanide/Pan-African-age, and Grenville-age populations comprise 14%, 23%, 14%, and 19% of the total, respectively. This sample exhibits three sharp Phanerozoic peaks of diminishing prominence at 158 Ma, 260 Ma, and 400 Ma, plus another prominent Neoproterozoic peak at 600 Ma. Broader subsidiary peaks, ordered by decreasing amplitude, occur at ca. 1060 Ma, 1440 Ma, 1200 Ma, 1660 Ma, 2110 Ma, and 2710 Ma.

4.2.3. Samples of Unknown Affinity

14CM21. This sample of sheared migmatitic gneiss of the Gold Flat amphibolite of either the upper portion of the outer CMS or the deepest portion of the Rattlesnake Creek terrane yielded a unimodal ca. 167–209 Ma spread of ages from 14 cathodoluminescent (CL)-dark, oscillatory-zoned zircon-core domains, from which a concordia age of 171.1 ± 1.6 Ma (2σ) was determined. Thin (<20 μm), CL-bright domains exist on nearly all grains analyzed; two analyses of such domains yielded relatively high-U/Th ratios (~5–7) and ages of 150.0 ± 2.1 Ma and 163.8 ± 3.3 Ma. The textures and geochemistry observed in zircon rims suggest that these domains are of metamorphic origin, though insufficient ages were determined for calculation of the timing of recrystallization.

19KM3. Respectively, YSP and MLA MDAs of 162.1 ± 0.4 Ma and 164.2 ± 0.4 Ma (1σ) were calculated from this sample, which yielded 184 concordant U-Pb zircon ages ranging from 150.6 ± 12.2 Ma to 2747.3 ± 13.4 Ma (1σ). This sample exhibits a dominant peak at ca. 166 Ma, with Jurassic grains comprising 48% of the total, and an auxiliary peak at ca. 260 Ma. Scattered Paleozoic (12%) peaks concentrated at ca. 350 Ma and 450 Ma, Grenville-age grains (6%) with a peak at ca. 950 Ma, and pre-Grenville-age grains with peaks at 1480 Ma and 1780 Ma comprise most remaining grains. Timanian/Pan-African grains are rare in this sample, comprising only 3%.

5. DISCUSSION

In this section, we address: (1) local geologic problems pertaining to the affinities of the Gold Flat amphibolite and schist exposed at the NE margin of the Klamath River appendage, (2) infer the ages and sources of the CMS to evaluate possible regional correlations, (3) discuss the mechanisms that likely controlled assembly of the CMS, and (4) provide a model for emplacement of the CMS in the context of Mesozoic plate motions.

5.1. Affinities of Samples of Unknown Origin

5.1.1. Affinity of the Gold Flat Amphibolite

The Gold Flat amphibolite was assigned by Barrows (1969) and Burton (1982) to the base of the Rattlesnake Creek terrane, in the upper plate of the Condrey Mountain shear zone, on the basis of structural position and the presence of garnet-bearing, amphibolite-facies assemblages. However, it is conceivable that the Gold Flat amphibolite represents the amphibolite-facies culmination of a documented north-to-south metamorphic field gradient that begins in greenschist-facies, outer CMS assemblages near the confluence of the Scott and Klamath rivers (Barrows, 1969; Saleeby and Harper, 1993). Indeed, our U-Pb data from oscillatory-zoned zircon-core domains from the Gold Flat amphibolite point to igneous crystallization of this unit at ca. 171 Ma (Fig. 6), an age that is ~20 m.y. younger than the youngest dated igneous protoliths from the Rattlesnake Creek terrane (cf. Wright and Wyld, 1994) and overlapping ages from igneous protoliths of the outer CMS. The "Scott River granophyre" of Saleeby and Harper (1993), a relatively large leucosome sampled from the Gold Flat amphibolite, yielded a slightly discordant multifraction age of 157 +3/–2 Ma, which these workers attributed to some combination of inheritance plus open-system behavior. New results from single zircon crystals extracted from the same leucosome material yield U-Pb ages of 155.3 ± 0.3 Ma (Gates et al., 2019). We interpret the array of ages determined from the Gold Flat amphibolite to reflect the mixing of igneous and metamorphic grain domains. The above lithologic and geochronologic relations strongly suggest that the Gold Flat unit does not belong to the Rattlesnake Creek terrane in the upper plate of the Condrey Mountain shear zone and instead represents migmatitic amphibolite-facies equivalents of the outer CMS. Alternatively, the Gold Flat amphibolite may represent an exposure of ca. 170 Ma intrusive material, such as the Vesa Bluffs pluton or Ironside Mountain batholith, which sporadically intrude the Rattlesnake Creek terrane.

5.1.2. Affinity of the NE Klamath River Appendage

Accurate regional tectonic models depend critically on the correct identification of rocks exposed along the NE margin of the Klamath River appendage (Figs. 1 and 2). The assertion of Hill (1984) that the inner CMS intervenes between the Galice Formation and China Peak Complex has significant implications for: (1) the relative age of the CMS, Galice Formation, and Nevadan orogeny, and (2) the magnitude of slip along Nevadan structures responsible for Galice burial.

Sample 19KM3 yields a Late Jurassic MDA and shows significant age-spectrum overlap with both the Galice Formation (LaMaskin et al., 2021; Surpless et al., 2024) and, to a lesser degree, the lens of semipelite within the outer CMS (sample 15KM23, this study; Figs. 7–9; Table 2). These samples are all characterized by significant populations of Jurassic ages (approximately half of the grains analyzed) and Paleoproterozoic and older ages, with low proportions of Paleozoic plus Timanian/Pan-African- and Grenville-age grains. The age spectra and MDAs derived from the inner CMS do not match those of sample 19KM3 as closely.

Hence, detrital zircon ages in sample 19KM3 are most compatible with a Klamath River appendage Galice and/or an outer CMS metasedimentary origin. The paleogeographic/tectonic scenario that led to similarities in detrital zircon age spectra among the Galice Formation of the Klamath River assemblage, outer CMS metasediments, and sample 19KM3 will be explored further in the sections that follow.

5.2. Age and Provenance of the Condrey Mountain Schist

5.2.1. Outer Condrey Mountain Schist

Igneous samples from the outer CMS yield U-Pb ages of ca. 171–170 Ma (Saleeby and Harper, 1993; this work; Fig. 6), which we interpret to reflect the timing of eruption and emplacement of mafic volcanic and intrusive protoliths. One detrital sample (15KM23), recovered from the "semipelite" interval of Helper (1985) in the center of the outer CMS, yields an MDA of ca. 170 Ma. Given the approximately unimodal Middle-to-Late Jurassic age peak derived from this sample, we infer that its hemipelagic protolith was sourced largely from the adjacent ca. 170 Ma Western Hayfork arc and possibly consanguineous China Peak Complex (discussed further in the following paragraph), with input of pre-Jurassic grains from the eastern Klamath Mountains Province or further inboard.

The outer CMS shares a similar range of lithologies with the China Peak Complex, for example, metamorphosed mafic volcanic and intrusive rocks and subordinate metasedimentary rocks and felsic dikes, an overlapping range of igneous ages, and an identical structural position beneath the Rattlesnake Creek terrane along a regional thrust fault. Alternatively, the Western Hayfork terrane may represent a suitable correlative to the outer CMS, given that each consists of ca. 170 Ma volcaniclastic strata and tuffaceous intervals of basaltic to andesitic composition. However, the China Peak Complex and Western Hayfork terrane may be consanguineous, and distinguishing between them is therefore futile. However, we consider a Western Hayfork terrane–outer CMS link less likely given that the Western Hayfork terrane resides structurally above the Rattlesnake Creek terrane (e.g., Donato, 1987; Saleeby and Harper, 1993; Barnes and Barnes, 2020).

Correlation of the outer CMS with underthrust China Peak assemblages leads us to infer the following paleogeographic setting for the formation of the outer CMS unit, which was adapted from Donato (1987) and Saleeby and Harper (1993).

At ca. 175 Ma, a few million years prior to formation of the outer CMS protoliths, the Klamath Mountains Province consisted of four terranes inboard of the Rattlesnake Creek terrane, upon which the Western Hayfork arc was being constructed. The arrangement of this framework plus the high-Mg andesitic and adakitic geochemistry of the Western Hayfork terrane likely reflects eastward subduction of young, hot Farallon oceanic lithosphere (Barnes and Barnes, 2020). At ca. 172 Ma, a phase of extension affected this framework, perhaps due to some combination of: (1) a rapid change in the absolute motion of North America (May and Butler, 1986; Saleeby and Harper, 1993); and (2) upper–lower plate coupling above an aging, and cooling, subducting Farallon plate (i.e., slab rollback). Extensional tectonism localized within the Western Hayfork and Rattlesnake Creek terranes, forming sheeted dikes of the China Peak and Preston Peak complexes and covering the region with volcaniclastic to hemipelagic sediment. Rifting was interrupted by the ca. 170 Ma Siskiyou event, which led to regional shortening and thrusting of the Western Hayfork terrane >15 km beneath the Sawyers Bar terrane, followed by minor thrusting of the Rattlesnake Creek terrane beneath the Western Hayfork terrane, and stitching of these terranes by batholith-scale intrusives (Wright, 1982; Wright and Fahan, 1988; Barnes and Barnes, 2020). At ca. 164 Ma, shortening waned and extension resumed, resulting in the generation of the Josephine ophiolite and hemipelagic precursors to the Galice Formation, while the Rogue-Chetco and Wooley Creek volcano-plutonic belts flanked the Josephine basin.

Following rifting and formation of the Josephine basin, extension yielded to shortening once again with the ca. 157 Ma onset of the Nevadan event. Cooling ages from the outer CMS and the base of the Rattlesnake Creek terrane strongly suggest that these units were juxtaposed at this time (Helper, 1985; Saleeby and Harper, 1993; Hacker et al., 1995). The presence of China Peak protoliths within the Condrey Mountain window requires at least 50 km of underthrusting along the Condrey Mountain shear zone. This shear zone juxtaposes the outer CMS with the exposed, rootless base of the Wooley Creek plutonic belt and its Rattlesnake Creek terrane framework. Removal of the base of the Wooley Creek belt and emplacement of the outer CMS with no intervening mantle strongly suggests that shearing must have occurred at an anomalously low angle. We suggest that the heat required for greenschist–upper amphibolite-facies metamorphism in the outer CMS and outboard equivalents in the China Peak Complex was supplied from the upper plate, which had been recently invaded by the 165–156 Ma Wooley Creek plutonic belt.

5.2.2. Inner Condrey Mountain Schist: Provenance

Metasedimentary rocks in the inner CMS, including both White Mountain and Dry Lake subunits, are lithologically similar and yield overlapping distributions of detrital zircon grains from structurally deep to shallow levels. All samples analyzed from the inner CMS exhibit a prominent Middle–Late Jurassic age peak that is centered at ca. 160 Ma. This Jurassic population was

most likely sourced from ca. 165–156 Ma plutons and ca. 156–152 Ma late-stage intrusives of the Wooley Creek belt (Hacker et al., 1995; Irwin and Wooden, 1999; Snoke and Barnes, 2006; MacDonald et al., 2006; Coint et al., 2013), with probable input from the ca. 161–155 Ma Rogue-Chetco arc and/or plagiogranite derived from underlying Josephine ophiolite basement (Harper et al., 1994). Additional contributions from eroded Jurassic plutons of the Sierra Nevada arc and retroarc are also likely, as Hf isotopic analysis of Middle–Late Jurassic grains extracted from the Galice Formation requires an origin outside of the Klamath Mountains Province (Surpless et al., 2024).

The majority of detrital zircon grains contained within the inner CMS are pre-Mesozoic, some of which (e.g., Paleoproterozoic and older grains) may be explained by westward shedding of material eroded from the Siskiyou and/or Nevadan orogenic highlands to the east (Figs. 8 and 9). However, it should be noted that the inner CMS contains higher proportions of Grenville-age and Permian–Triassic detrital zircon grains and lower proportions of Paleoproterozoic grains than are observed in pre-CMS assemblages of the Klamath Mountains, such as the Fort Jones/Stuart Fork and Sawyers Bar terranes (Scherer and Ernst, 2008; Scherer et al., 2010; Ernst, 2017). Furthermore, the inner CMS contains distinct Paleozoic and Timanian/Pan-African age peaks, centered at 400 Ma and 600 Ma, respectively.

These relations require inmixing of at least one additional source component containing abundant Grenville-age, Permian–Triassic, Paleozoic, and Timanian/Pan-African-age detrital zircon grains. Recycled Triassic backarc basin strata of Nevada and eastern California (Manuszak et al., 2000; Darby et al., 2000; Gehrels and Pecha, 2014; Dickinson and Gehrels, 2008; LaMaskin et al., 2011) and/or Jurassic erg materials of the Colorado Plateau and adjacent areas (e.g., Dickinson and Gehrels, 2003, 2009) are excellent candidates for the extraregional input(s) required to fully explain detrital zircon age spectra of the inner CMS. Incorporation of one or both of these components likely involved erosion in the backarc region, perhaps within the Luning-Fencemaker thrust belt (e.g., Wyld, 2002; Wyld et al., 2003) or the Mogollon Highlands (Mauel et al., 2011), and westward routing of the resulting detritus along the flanks of the elevated Klamath–northern Sierra Nevada Mountains before entering the Josephine basin. This recycled backarc signal observed in the inner CMS is likewise noted in clastic materials of the Franciscan Eastern belt, the Galice Formation, and the basal Great Valley Group. This detrital component was, therefore, ubiquitous within the Late Jurassic–Early Cretaceous forearc realm, and strongly suggests the arc was not yet prominent enough to block detritus from the continental interior (DeGraaff-Surpless et al., 2002; Surpless et al., 2006, 2024; Dumitru et al., 2010; Orme and Surpless, 2019; LaMaskin et al., 2021; Figs. 8 and 9).

Early Cretaceous detrital zircon grains are found only at deep structural levels of the inner CMS. These grains most likely originated from some combination of two sources: (1) ca. 142–136 Ma plutons of tonalitic to granodioritic composition (Snoke and Barnes, 2006) that are exposed throughout the Klamaths, and/or (2) volcanic ash that erupted from the ca. 130–140 Ma westernmost edge of the Sierran arc, which is now largely buried beneath Great Valley forearc basin strata (Saleeby, 2007). An airfall origin for ca. 137 Ma and younger zircon in the South Fork Mountain schist is inferred by Dumitru et al. (2010) based on the abundance of very small grains of these ages in radiolarian chert, a rock type that is not known for incorporating significant clastic material.

Some models for the Jurassic to Cretaceous tectonic evolution of the Klamath Mountains Province call on collision of the southern flank of the Wrangellia-Alexander composite terrane (e.g., Tipper, 1984; Wernicke and Klepacki, 1988; McClelland et al., 1992). This model predicts some detrital contributions from the Wrangellia-Alexander terrane to sediment being deposited in intervening basins (e.g., the Galice Formation, the South Fork Mountain schist [SFMS], and the CMS) during its approach. Recent detrital zircon geochronology from late Paleozoic strata of the southern Wrangellia-Alexander terrane, exposed on Vancouver Island (British Columbia, Canada), reveals abundant Carboniferous ages (ca. 344–317 Ma) and very few pre-400 Ma grains (Alberts et al., 2021). This Carboniferous component is not recognized in the Galice formation, SFMS, or CMS, which suggests that either Paleozoic strata of the Wrangellia-Alexander terrane were not exposed during collision, that Wrangellia-Alexander terrane-derived sediment was not shed toward the Klamath Mountains Province, or that the terrane did not collide at the paleolatitude of the Klamath Mountains in the Jurassic to Cretaceous time frame.

5.2.3. Inner Condrey Mountain Schist: Age

Structurally shallow samples (i.e., subjacent to the Condrey internal fault and in the vicinity of White Mountain; Fig. 2) yield older MDAs than those from the Dry Lake area (ca. 160–153 Ma versus ca. 143–130 Ma; Table 2; Fig. 10). It is conceivable that the entire inner CMS pile was deposited synchronously and that the local environment in which structurally shallow samples were deposited did not receive significant quantities of Early Cretaceous detrital zircon. We consider this unlikely, since K-Ar white mica ages vary from ca. 141 Ma beneath the Condrey internal fault to ca. 128 Ma in the Dry Lake area (Lanphere et al., 1968; Helper, 1985). These age relations suggest that the outermost portion of the inner CMS was buried, grew metamorphic white mica, and cooled through K-Ar closure prior to deposition of Dry Lake area protoliths. We suggest that samples directly beneath the Condrey internal fault represent a package of material that is distinct from that observed at deeper structural levels. In reality, the inner CMS is likely composed of more than two tectonic slices, as noted by Tewksbury-Christle et al. (2021), though sheared boundaries separating packages have not been directly observed, perhaps due to poor exposure or because they are gradational. Coupling Ar-Ar thermochronology with detrital zircon U-Pb geochronology would provide a means of resolving additional slices if they are present. Regardless, regional correlation of the inner CMS and its subunits has significant implications for the late Mesozoic tectonic development of the Klamath Mountains Province.

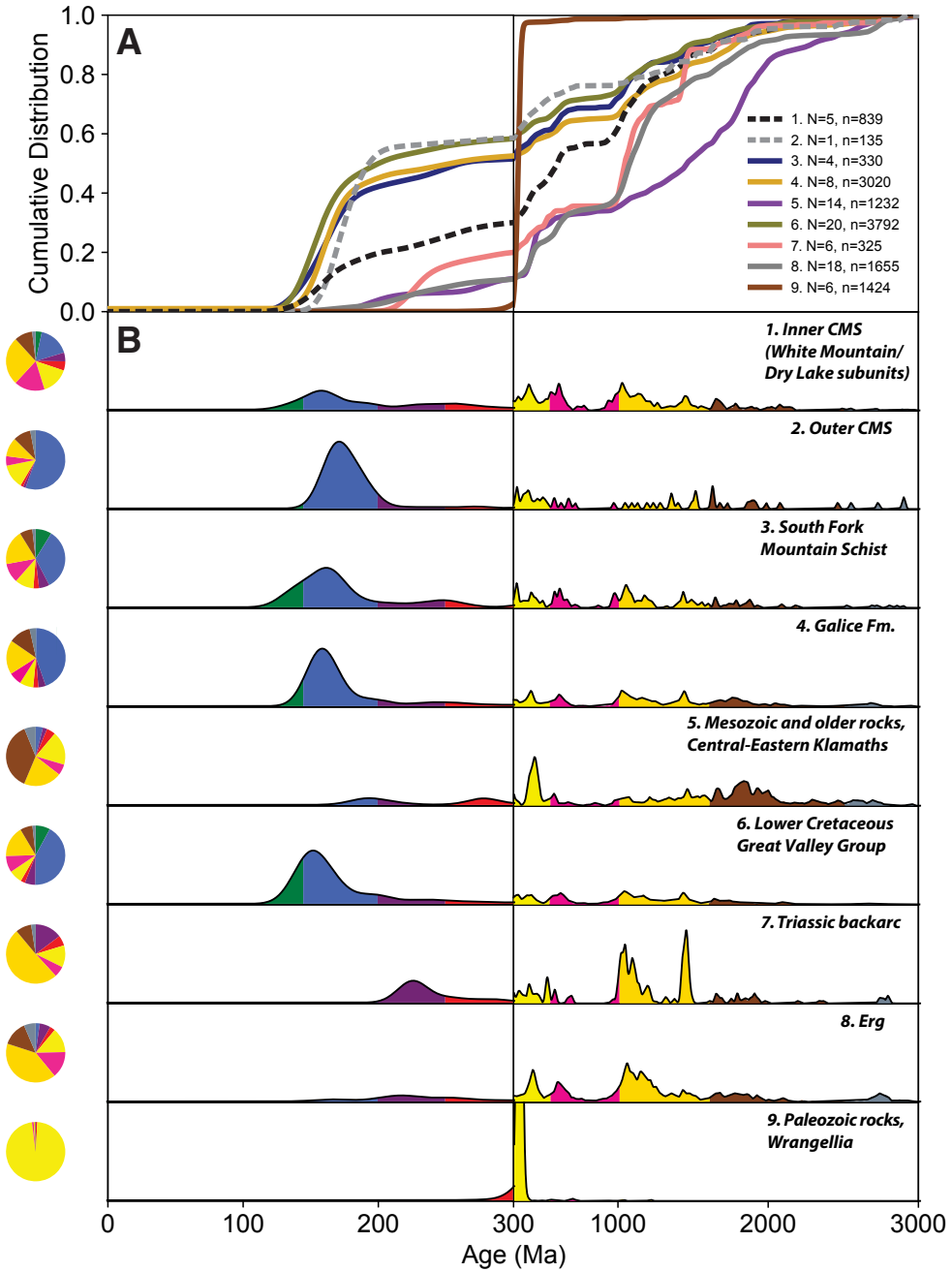

Figure 8. (A) Cumulative probability plot, and (B) corresponding normalized kernel density estimates (KDEs) with 10 m.y. bandwidth comparing detrital zircon ages from samples collected from forearc, arc, and backarc domains of the Middle Jurassic–Early Cretaceous Klamath Mountains Province. Note the split horizontal axis at 300 Ma and that spectra between 300 Ma and 3000 Ma are vertically exaggerated by a factor of five. Numbers in part A correspond to those adjacent to curves in part B. Pie diagram bin colors correspond to those beneath each KDE curve. Abbreviations: N—number of samples analyzed; n—number of concordant grains analyzed. Data sources: 1 and 2—this study; 3—Dumitru et al. (2010), Chapman et al. (2021b); 4A—LaMaskin et al. (2021), Surpless et al. (2024); 5—Gehrels and Miller (2000), Wallin et al. (2000), Grove et al. (2008), Scherer and Ernst (2008), Scherer et al. (2010), Ernst et al. (2017); 6—Orme and Surpless (2019); 7—Manuszak et al. (2000), Darby et al. (2000), Gehrels and Pecha (2014); 8—Dickinson and Gehrels (2009); 9—Alberts et al. (2021). CMS—Condrey Mountain schist.

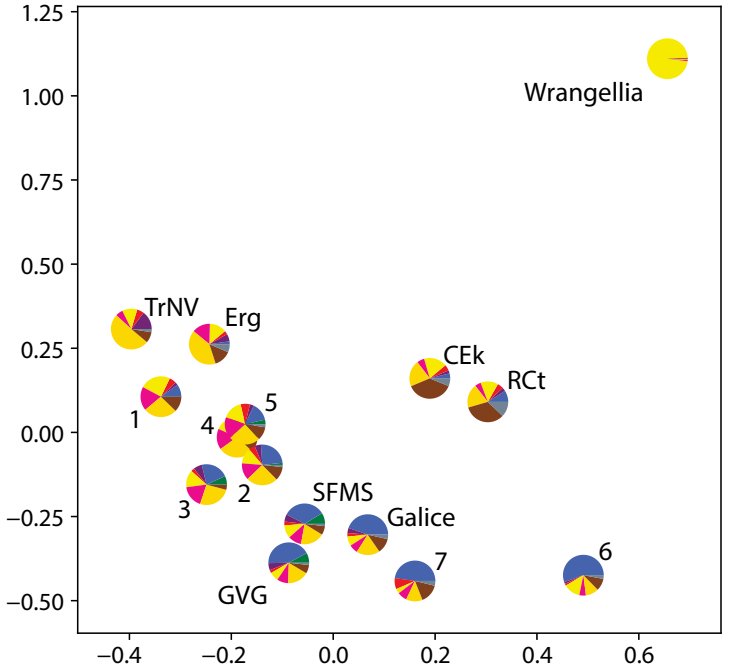

Figure 9. Multidimensional scaling plot with samples plotted as pie diagrams. Pie diagram bin colors correspond to those beneath kernel density estimate curves in Figures 7 and 8. Axes are dimensionless D_{max} distances (Vermeesch, 2013). Data sources: samples 1–7 (Tables 1 and 2)—this study; Mesozoic and older rocks of the central and eastern Klamath Mountains (CEk)—Gehrels and Miller (2000), Wallin et al. (2000), Grove et al. (2008), Scherer and Ernst (2008), Scherer et al. (2010), Ernst et al. (2017); Erg—Dickinson and Gehrels (2009); Galice Formation (Galice)—LaMaskin et al. (2021), Surpless et al. (2024); Great Valley Group (GVG)—Orme and Surpless (2019); Rattlesnake Creek terrane cover (RCt)—LaMaskin et al. (2021); South Fork Mountain schist (SFMS)—Dumitru et al. (2010); Triassic backarc rocks (TrNV) and Wrangellia—Alberts et al. (2021).

5.2.4. The Inner CMS: Galice or Franciscan?

The protoliths of the inner CMS, lower hemipelagic section of the Galice Formation, and the SMFS each consist chiefly of argillite and chert and therefore do not facilitate regional correlation. However, the abundance of turbidite in the upper portion of the Galice Formation and its absence from the CMS window render correlation of these units unlikely.

The structurally deep Dry Lake area contains the youngest material of the CMS. Detrital zircon age spectra and Early Cretaceous MDAs calculated from this area overlap those from the SFMS (Dumitru et al., 2010; Chapman et al., 2021b). This observation, in addition to structural and lithologic similarities between these units, strongly suggest that this portion of the CMS represents Franciscan assemblages displaced ~100 km inboard of the nearest previously recognized exposures of South Fork Mountain schist.

The structurally shallow White Mountain area yields MDAs older than those of structurally deep samples and overlapping those reported for the Galice Formation (LaMaskin et al., 2021; Surpless et al., 2024). However, the detrital zircon age spectra of White Mountain subunit samples more closely overlap those of the Dry Lake subunit and SFMS than those of the Galice Formation. For these reasons, we consider a White Mountain CMS–Galice correlation unlikely.

It is conceivable that sedimentary protoliths in the White Mountain area were deposited synchronously with those in the Dry Lake area, with the former not receiving detrital zircons of Early Cretaceous age. Indeed, Tewksbury-Christle et al. (2024) document a minute quantity (<1%) of Early Cretaceous detrital zircon grains within the White Mountain subunit.

Alternatively, the White Mountain area may represent a slice of pre-SFMS Franciscan, perhaps the Skaggs Springs schist. The Skaggs Springs schist of the Franciscan eastern belt represents a possible precursor to the much more voluminous, yet comparable metamorphic-grade South Fork Mountain schist (Dumitru et al., 2010). Compared to the South Fork Mountain schist, the Skaggs Springs schist yields an older MDA (ca. 144 Ma) and a younger main age peak (ca. 152 Ma versus 162 Ma; Snow et al., 2010). Notably, however, these differences are based on just 38 analyses available from the Skaggs Springs schist, which renders the relationships among the inner CMS and these important Franciscan units uncertain.

One could argue that the inner CMS is not equivalent to the SFMS, as the former yields older (141–128 Ma; Helper, 1985) white mica K-Ar ages than Ar-Ar ages from the latter (ca. 123 Ma; Dumitru et al., 2010). However, this difference may result from limited data (three or fewer samples from both units) and/or the indirect comparability of data sets (K-Ar versus Ar-Ar).

It is also possible that the CMS represents SFMS protoliths that subducted a few million years earlier than the remainder of the SFMS. Our favored interpretation, explored in the sections that follow, is that the CMS was emplaced during a phase of shallow-angle subduction with limited strike-parallel extent. Such an episode could conceivably result in localized CMS subduction prior to regional SFMS emplacement. Furthermore, the presence of Franciscan assemblages in the Condrey Mountain window, which likely continued at least ~50 km east of the window (observed as an ~3-km-thick, low-velocity layer; Fuis et al., 1987), requires significant low-angle underthrusting of subduction-accretion assemblages.

5.3. Middle–Late Jurassic Tectonic Evolution of the Klamath Mountains Province and Emplacement of the Outer Condrey Mountain Schist

The CMS appears to be a composite of three distinct units. First, emplacement of the outer CMS subunit, which is inferred to be greenschist–amphibolite-grade equivalents of the China Peak Complex, beneath the Rattlesnake Creek terrane most likely occurred during the Nevadan event.

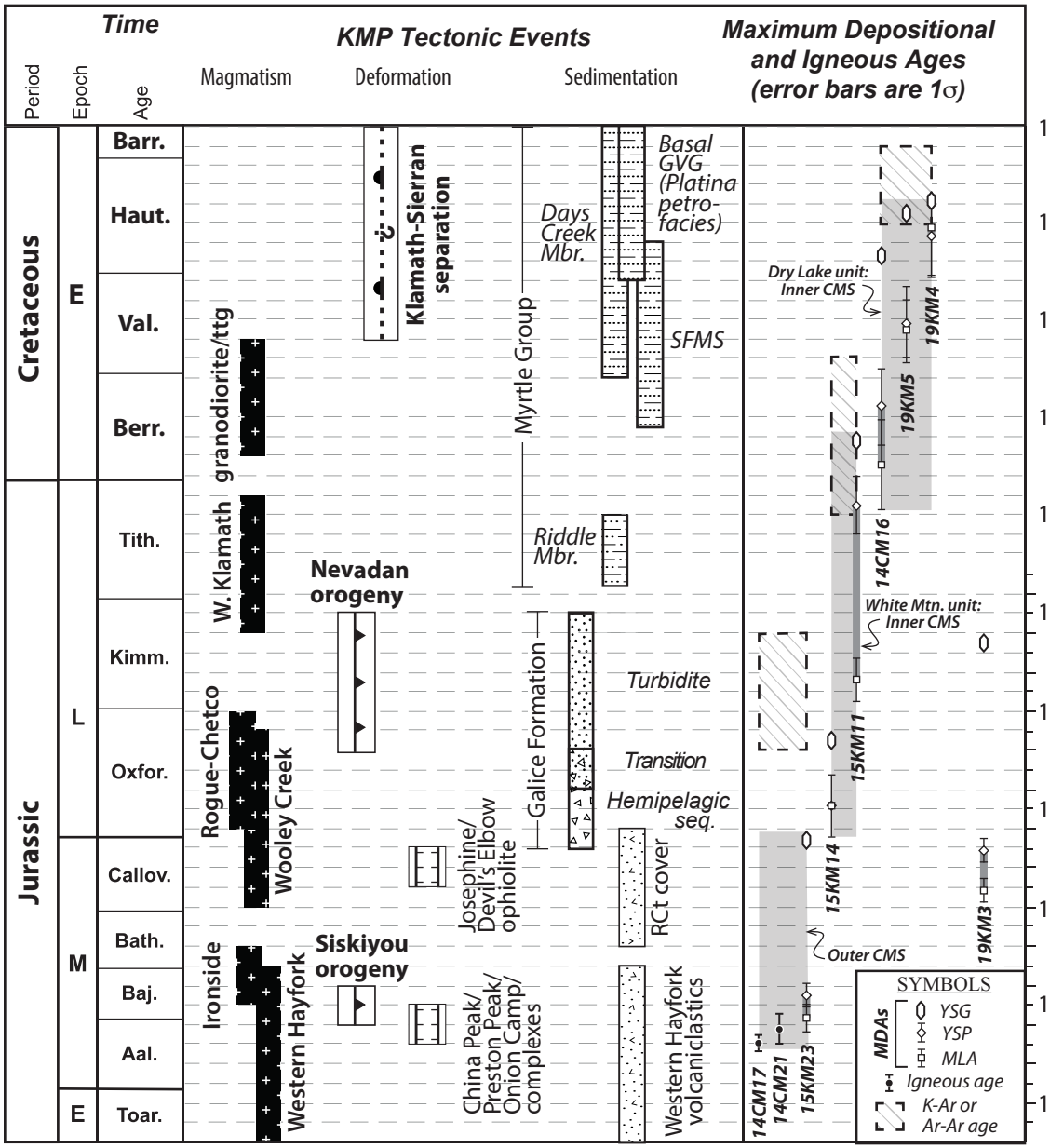

Figure 10. Summary of regional ages and events as well as maximum depositional ages from this study. Timing of Klamath Mountains Province (KMP) tectonic events was compiled from sources given in the text. Maximum depositional ages and associated uncertainties are from Table 2. YSG—youngest single grain; YSP—youngest statistical population; MLA—maximum likelihood algorithm. Igneous ages are from U-Pb zircon analysis (see Fig. 6). Jurassic and Cretaceous boundary ages are from Gradstein et al. (2020). E—Early; M—Middle; L—Late; CMS—Condrey Mountain schist; GVG—Great Valley Group; SFMS—South Fork Mountain schist RCt—Rattlesnake Creek terrane; Barr.—Barremian; Haut.—Hauterivian; Val.—Valanginian; Berr.—Berriasian; Tith.—Tithonian; Kimm.—Kimmeridgian; Oxfor.—Oxfordian; Callov.—Callovian; Baj.—Bajocian; Bath.—Bathonian; Aal.—Aalenian; Toar.—Toarcian.

Next, a section of probable eastern Franciscan belt equivalents (White Mountain subunit) underthrust the outer CMS after ca. 153–144 Ma (Table 1), possibly in the waning stages of the Nevadan event. Assembly of the CMS culminated with tectonic underplating of the innermost Dry Lake CMS subunit of Franciscan affinity, which is constrained to the interval between MDAs of ca. 140 Ma and ca. 128 Ma K-Ar cooling ages. We explore the tectonic implications of this apparent three-stage emplacement history of the CMS below.

Regional tectonism was clearly very dynamic preceding and during underthrusting of the outer and White Mountain subunits of the CMS and involved rapid changes from extension and formation of the China Peak Complex to shortening (Siskiyou phase), which was followed again by extension (Josephine basin formation) and culminated with convergence (burial of the outer CMS, Western Klamath terrane, and the White Mountain unit of the inner CMS). Notably, the change from ca. 170 Ma Siskiyou convergence to ca. 164 Ma Josephine extension to ca. 157 Ma Nevadan convergence over a brief time interval has long been recognized (e.g., Wright and Fahan, 1988; Hacker and Ernst, 1993; Snoke and Barnes, 2006). However, current models for the Jurassic tectonic development of the Klamath Mountains Province face challenges in explaining the swift transitions between periods of contraction and extension, as well as the spatial restriction of deformation.

The driver(s) of Siskiyou and Nevadan events are unclear, with debate surrounding the relative roles of changes in plate motion versus the collision of exotic lithosphere, namely the Wrangellia-Alexander superterrane. Changes in the rate and/or orientation of convergence between western North America and the Panthalassan realm at ca. 170 Ma and 150 Ma (e.g., May et al., 1989; Seton et al., 2012) have been invoked to explain Siskiyou and Nevadan deformation. If a global plate reorganization did indeed occur, why was deformation localized to a <500-km-long domain of the margin? Shouldn't the Siskiyou and/or Nevadan events have lasted longer? Shouldn't these events have been bracketed and interrupted by similarly brief and localized extensional episodes? Similar challenges arise with collisional models, as modern (e.g., the Alpine and Himalayan) and ancient (e.g., the Grenville, Appalachian-Caledonian, and Laramide) examples span thousands of kilometers and several tens of millions of years. Furthermore, recent U-Pb detrital zircon geochronology from the Rattlesnake Creek and Western Klamath terranes strongly suggests a western North America-fringing origin for these terranes, which rules out the possibility that they represent far-traveled materials such as a portion of the Wrangellia-Alexander superterrane (LaMaskin et al., 2021).

In light of the issues noted in the above paragraph, with models invoking changes in plate motion or superterrane collision, we suggest that rapidly alternating periods of localized extension and shortening are better understood in the context of "tectonic switching" (Collins, 2002). In this context, the Siskiyou event was preceded by a brief ca. 172 Ma extensional episode, as evidenced by sheeted dike complexes of the Preston Peak and China Peak complexes and the diverse array of magmas (Barnes and Barnes, 2020) generated in the Western Hayfork (extensional?) arc. Extensional tectonism may have been related to slab retreat and/or oceanward stepping of subduction (e.g., Donato, 1987). The Siskiyou event occurred at ca. 170 Ma with docking of fringing Rattlesnake Creek and Western Hayfork terranes. Encroachment of these terranes with earlier accreted materials was most likely accomplished through subduction of a small (less than a few hundred kilometers in diameter), yet buoyant and rough oceanic feature (e.g., a plateau, aseismic ridge, seamount chain, or fracture zone) embedded in subducting Panthalassa lithosphere, which would have enhanced basal traction along the subduction interface. Subduction of relatively smooth and thin oceanic lithosphere followed shortly after passage of this hypothetical oceanic feature; ensuing slab retreat induced an ~5 m.y. phase of upper-plate extension and formed the Josephine basin. Relatively steep subduction enabled asthenospheric counterflow and devolatilization melting, leading to magmatism in the Wooley Creek plutonic belt and Rogue-Chetco arc. At ca. 157 Ma (the Nevadan event), upper-plate magmatism waned, and extension yielded to shortening due to subduction of another buoyant and rough oceanic feature, underthrusting the outer CMS and the Western Klamath terrane. The punctuated and localized effects of impingement of multiple small oceanic features with the Middle–Late Jurassic margin of North America at the paleolatitude of the Klamath Mountains finds analogs in modern rough patches of subducting oceanic lithosphere, such as the Australian and Philippine Sea plates (LaMaskin et al., 2011; Lallemand et al., 2018). Alternatively, buckling of the downgoing slab along mantle-density interfaces may have played an additional role (e.g., Schellart and Strak, 2021).

In summary, the Jurassic evolution of the Klamath Mountains Province exhibits the hallmark traits of a region that has experienced tectonic switching, namely localized and rapidly alternating contraction and extension. An argument could be made, though, that the rough patches of seafloor crucial for tectonic switching were subducted into the mantle, rendering the model untestable. However, a fragment of the Middle Jurassic seafloor is preserved in the Rattlesnake Creek terrane. The existence of dismembered ophiolitic mélange in the Rattlesnake Creek terrane strongly suggests that the seafloor being conveyed toward the North American margin was a highly irregular surface.

5.4. Shallow-Angle Subduction Model for Early Cretaceous Assembly of the Inner Condrey Mountain Schist, Franciscan Accretion, and Klamath-Sierran Separation

Magmatism resumed as deformation associated with the Nevadan orogeny waned, permitting intrusion of primarily mafic magmas belonging to the ca. 151–144 Ma western Klamath suite (Barnes et al., 2006). Following intrusion of the western Klamath suite, the locus of magmatism migrated slightly (a few tens of kilometers) eastward and evolved toward more felsic compositions (ca. 142–136 Ma tonalite–trondhjemite–granodiorite and granodioritic suites; Barnes et al., 1992). Magmatism in the Klamath Mountains Province abruptly terminated at ca. 136 Ma (Allen and Barnes, 2006).

We infer the relations described above to have resulted sequentially from: (1) post-Nevadan slab rollback and associated extensional magmatism within

the opening mantle wedge; (2) slab shallowing and related arc migration plus incorporation of previously subcreted materials (e.g., Allen and Barnes, 2006); and (3) shallow/flat subduction, impingement, and/or removal of the circulating mantle wedge, and arc shutdown. Shortly after the cessation of magmatism, several additional noteworthy events occurred in the Klamath Mountains Province (Figs. 10 and 11).

First, the continental margin transitioned from non-accretion to an accretionary mode marked by the emplacement of the oldest slices of Franciscan Complex (i.e., the SFMS) beneath the Klamath Mountains Province along the Coast Range fault (Dumitru et al., 2010; Chapman et al., 2021b). These authors argue, based on observations from modern forearcs (e.g., Clift and Vannucchi, 2004; Scholl and von Huene, 2007), that accretion began in response to an increase in sedimentary flux into the trench. They conclude that the mechanisms driving increased sedimentation are unclear but may relate to an increase in magmatic flux in the Sierra Nevada batholith, erosion of orogenic highlands, and/or changes in relative plate motion.

It is difficult to envision the localized (i.e., Klamath Mountains Province-adjacent) increase in sedimentation required for Franciscan and inner CMS accretion as being driven by regional- (i.e., Sierra Nevada-scale) to global-scale phenomena. Instead, we speculate that localized (no more than a few hundred kilometers along orogenic strike), shallow-angle subduction led to increased basal traction along the margin, which led to growth of the accretionary wedge and an increase in underplating. Correlation of the inner CMS Dry Lake subunit with the SFMS requires that the former accumulated in the Early Cretaceous trench and underthrust the Klamath Mountains Province along the equivalent of the Coast Range fault. The shallowly dipping tectonic contact separating the Klamath Mountains Province basement and lower-plate inner CMS requires tectonic erosion of formerly intervening mantle lithosphere.

Second, the Klamath Mountains Province relocated westward from the axis of arc magmatism to the forearc domain and was affected by extension (Constenius et al., 2000; Batt et al., 2010a, 2010b; Ernst, 2013). Ernst (2013) invokes a decrease in upper–lower plate coupling to explain these relations, speculating that a change in subducting material from old (i.e., cold and thick) to young (i.e., warm and thin) oceanic lithosphere may be responsible. We concur that extension and westward motion of the Klamath Mountains Province likely involved a reduction of interplate coupling. However, there are no modern analogs for subduction of a <200-km-wide patch of young oceanic lithosphere flanked by significantly older lithosphere, except where spreading ridges are colliding with continental margins; if a spreading center had collided with the Klamath Mountains Province in Early Cretaceous time, evidence for an elevated geothermal gradient at that time should be present. Instead, we suggest that slab rollback from the originally shallower trajectory profoundly reduced upper–lower plate coupling, facilitating trench retreat, westward displacement of the Klamath Mountains Province, and extension within the province.

The proposed Early Cretaceous shallow-angle subduction episode and ensuing rollback mark the final events of more than 50 m.y. of tectonic switching experienced by the Klamath Mountains Province. To summarize, two pronounced cycles of tectonic switching include: (1) ca. 175–170 Ma extension, during which the China Peak Complex, Western Hayfork arc, and outer CMS protoliths formed followed by the ca. 170 Ma Siskiyou event, and (2) ca. 164–162 Ma extension and formation of the Josephine basin followed by the ca. 157–151 Ma Nevadan event. A relatively feeble third event is marked by ca. 151–144 Ma formation of western Klamath suite magmas, slab shallowing, and inboard migration of magmatism, and ca. 140–128 Ma shallow-flat slab emplacement of the Dry Lake subunit of the inner CMS. A final phase of extension in the Klamath Mountains Province, and associated deep-marine sedimentation, accompanied its westward translation in the ca. 136–125 Ma window (Ernst, 2013).

5.5. What Is Franciscan, and What Portions of the Condrey Mountain Schist Qualify?

Hallmarks of the Franciscan Complex, summarized by Berkland et al. (1972) and Wakabayashi (2015), include: (1) the presence of diverse lithologies, consisting chiefly of metamorphosed clastic sedimentary rocks with lesser amounts of serpentinite, basalt, chert, and limestone; (2) metamorphism along a high-pressure/low-temperature array, generally spanning the zeolite, prehnite–pumpellyite, blueschist, and eclogite facies; (3) depositional and metamorphic ages spanning Early Cretaceous to Paleogene time; (4) its presence beneath Middle to Late Jurassic ultramafic rocks, gabbro, and basalt of the Josephine ophiolite in Northern California/southern Oregon and the Coast Range ophiolite in more southerly California; and (5) a variety of structural styles from generally coherent to internally broken to mélange.

The Dry Lake subunit meets all criteria listed above, contains an array of rock types similar to that of the South Fork Mountain schist, and MDAs and detrital zircon age spectra from the South Fork Mountain schist and Dry Lake subunit overlap significantly. The White Mountain subunit is likewise lithologically identical to the South Fork Mountain Schist and Dry Lake subunit. However, despite hosting detrital zircon grains yielding a similar array of ages as those of the South Fork Mountain schist and Dry Lake subunit, the White Mountain subunit yields older MDAs. Age constraints on the emplacement of this subunit are virtually absent, with small quantities of Early Cretaceous detrital zircon grains (Tewksbury-Christle et al., 2024) and a single white mica K-Ar age of ca. 144 Ma reported (Lanphere et al., 1968), which raises the possibility that this subunit indeed accreted in Early Cretaceous time. Is the White Mountain subunit of the inner CMS Franciscan? The only apparent reason to exclude the subunit appears to be on the basis of its age. For this reason, we recommend that the White Mountain subunit of the inner CMS be considered Franciscan.

Reimagining the entire inner CMS as Franciscan has implications for what controlled the accretion of clastic units in the Franciscan, as the inner CMS may represent the oldest known slice of predominantly sedimentary material contained in the Franciscan Complex. If, as we suggest, emplacement of the inner CMS was controlled by one or more episodes of shallow-angle

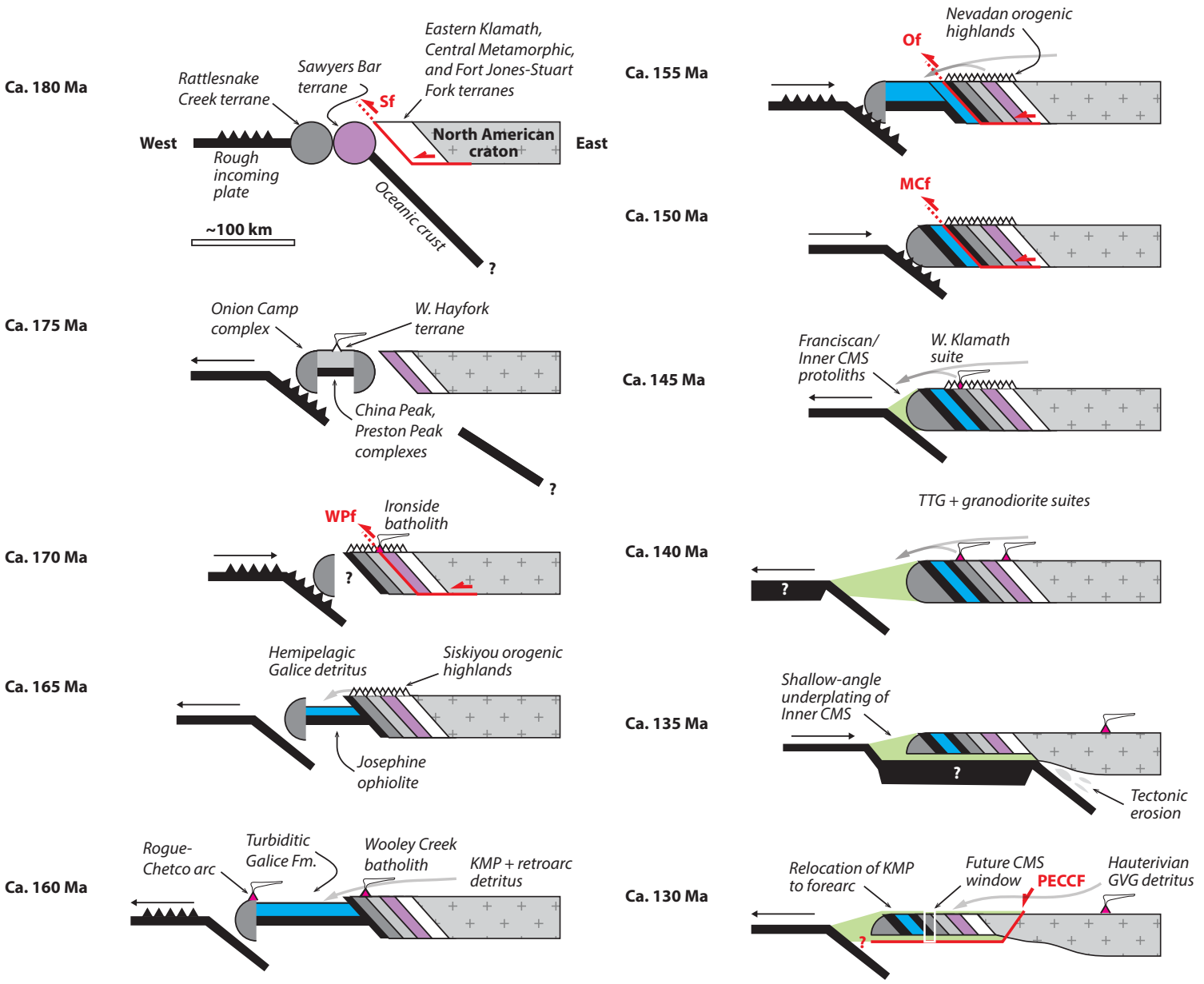

Figure 11. Model for Middle Jurassic to Early Cretaceous development of the Klamath Mountains Province (KMP). At 180 Ma, Sawyers Bar terrane and outboard Rattlesnake Creek terrane dock with previously accreted Eastern Klamath, Central Metamorphic, and Fort Jones–Stuart Fork terranes. Slip occurs along Siskiyou fault (Sf). At 175 Ma, trench retreats due to decreased upper–lower plate coupling. Onion Camp Complex rifts from Rattlesnake Creek terrane, producing Preston Peak and China Peak mafic complexes. Western Hayfork arc initiates. At 170 Ma, trench advances and coupling drives Siskiyou orogeny and slip along the Wilson Point fault (WPf); invasion of Ironside batholith closely postdates deformation. At 165 Ma, trench retreats due to reduced coupling. Trench retreat initiates upper-plate extension and formation of the Josephine ophiolite. Hemipelagic section of Galice formation, sourced primarily from the KMP, fills Josephine ophiolite-floored basin. At 160 Ma, extension and associated ophiolite formation and basin filling continue, and upper-plate magmatism flanks the east (Wooley Creek) and west (Rogue-Chetco) sides of the ophiolite-floored basin. At 155 Ma, rifting and arc magmatism each terminate as upper–lower plate coupling increases, driving the Nevadan event and thrusting along the Orleans fault (Of). KMP-derived and extraregional detritus fills the Josephine ophiolite-floored basin as the basin closes. At 150 Ma, Nevadan deformation culminates with thrusting along the Madstone Cabin fault (MCf). At 145 Ma, the predominantly mafic Western Klamath suite ignites as local and extraregional detritus continues to accumulate along the margin, forming the proto-Franciscan/Inner Condrey Mountain schist (CMS) accretionary wedge. At 140 Ma, the trench continues to roll back and intermediate magmatism (tonalite-trondhjemite-granodiorite, or TTG) occurs across the KMP. Franciscan/Inner CMS detritus continues to accumulate in the growing wedge. At 135 Ma, protoliths of the CMS begin underthrusting the KMP at low-angle, removing the lower crust via tectonic erosion; the driver of shallow-angle subduction is unknown. Thickened oceanic lithosphere is offered as a possibility. At 130 Ma, the trench rolls back, precipitating upper-plate normal faulting along the Paskenta/Elder Creek/Cold Fork (PECCF) fault, which was possibly facilitated by removal of isostatically compensating lower crust in the 135 Ma panel, and relocating the KMP from the arc to the forearc. Basal Great Valley Group (GVG) detritus blanket the subdued Early Cretaceous topography of the KMP.

subduction, then the switch from non-accretion to accretion (e.g., Dumitru et al., 2010) may have been flipped as the slab shallowed.

Is the outer CMS Franciscan? This unit contains chiefly basaltic flows and pyroclastic deposits metamorphosed under greenschist- to amphibolite-facies conditions in Middle to Late Jurassic time, which is at odds with the Franciscan characteristics listed at the beginning of this section. Furthermore, the structural relationship between the outer CMS and the Josephine ophiolite is unclear, as the outer CMS probably represents the buried equivalents of early rift products. If the outer CMS does indeed represent a buried early rift facies of the Josephine ophiolite, then protoliths of the outer CMS were likely emplaced in and erupted onto marginal North American crust, notably distinct from the trench setting in which the Franciscan Complex formed. These relations lead us to suggest that the outer CMS does not belong to the Franciscan Complex. However, burial of the ophiolitic upper plate to the Franciscan Complex appears to be restricted to the outer CMS and broadly correlative Josephine ophiolite of the Klamath Mountains Province, as the Coast Range ophiolite of more southerly California did not experience burial-related metamorphism exceeding zeolite grade (Evarts and Schiffman, 1983). Such burial and accretion of the outer CMS, while distinct in character from the Franciscan Complex, marked the end of a protracted phase of non-accretion and heralded the arrival of the first packages of Franciscan assemblages.

5.6. A Comparison with the Pelona–Orocopia–Rand and Related Schists of Southern California and Arizona

The Late Cretaceous–early Cenozoic Pelona–Orocopia–Rand and related schists of Southern California and Arizona represent the world's best-known example of the exhumed products of shallow-angle subduction (e.g., Saleeby, 2003; Jacobson et al., 2007; Chapman, 2017). Five key observations, summarized by Ducea et al. (2009) and Chapman (2017), reveal the tectonic significance of the Pelona–Orocopia–Rand schist. First, the schist consists chiefly of continent-derived immature clastic material with subordinate oceanic rocks—typical subduction-accretion assemblages—residing beneath continental arc plutons of the continental interior. Second, the contact between these rock packages is a shallow-angle ductile structure that separates lower-plate schist and upper-plate arc assemblages. Third, the lower plate exhibits an inverted metamorphic field gradient and achieves peak temperatures of ~100 °C lower than the overriding plate. Fourth, the depositional and metamorphic ages of lower-plate clastic materials broadly overlap with the intrusive ages of upper-plate plutons, which requires underthrusting at plate tectonic rates. Finally, outside of the schist outcrop belt, the arc is separated from subduction-accretion assemblages (i.e., the Franciscan Complex to the north and Western Baja terrane to the south) by a forearc basin underlain by ophiolitic basement and subcontinental mantle lithosphere. In other words, the lateral extent of shallow-angle, subduction-related damage is apparently restricted to the schist domain, where forearc lithosphere is absent.

Saleeby (2003) argue, based on observed margin-parallel tectonostratigraphic variations, that Late Cretaceous subduction along the western margin of North America consisted of normally dipping domains interrupted by a shallowly dipping segment in Southern California. This argument was later bolstered by forward and inverse geodynamic modeling that strongly suggested a conjugate to the Shatsky Rise of the NW Pacific Ocean basin collided with Southern California in Late Cretaceous time (Liu et al., 2010).

The CMS satisfies all shallow-angle subduction criteria, with one caveat. Like the Pelona–Orocopia–Rand schist, the CMS contains chert plus mafic and ultramafic rocks of oceanic origin. However, the Pelona–Orocopia–Rand schist and CMS are dominated by psammitic and hemipelagic protoliths, respectively. This key difference reflects deposition of Pelona–Orocopia–Rand schist protoliths proximal to the continent, probably along the trench slope, whereas CMS protoliths probably represent more distal trench-floor deposits. Some combination of the following factors probably led to this key lithologic difference: (1) a higher sedimentation and/or plate convergence rate for the case of the Pelona–Orocopia–Rand schists or (2) the presence of basement highs or lows that blocked coarse clastic material from becoming part of the CMS section (e.g., Underwood et al., 1980; Engebretson et al., 1984).

One additional hallmark of shallow-angle subduction, noted by Coney and Reynolds (1977) in the SW North American Cordillera, is a migrating locus of magmatism that sweeps inboard during slab shallowing. For the case of the Klamath Mountains Province, the relative positions of Latest Jurassic and Early Cretaceous plutons imply relatively modest arc migration within this time frame (a few tens of kilometers; Snoke and Barnes, 2006). However, the entire Klamath Mountains Province moved off the axis of magmatism in Early Cretaceous time, separating from the Sierran arc, to reside ~200 km to the west in the forearc realm (e.g., Ernst, 2013). Therefore, if magmatism at the latitude of the Klamath Mountains Province indeed continued from Early into Middle Cretaceous time, then the products of said magmatism would be expected east of the Klamath Mountains Province. Unfortunately, basement rocks east of the Klamath Mountains Province are covered by several kilometers of sedimentary and volcanic rocks, including the Upper Cretaceous Hornbrook Formation, Paleogene volcaniclastic rocks of the Payne Cliffs and Colestin formations, and Plio-Quaternary volcanic rocks of the Cascade Range and Modoc Plateau provinces (Berge and Stauber, 1987; Fuis et al., 1987; Guffanti et al., 1996). To our knowledge, no basement-derived xenoliths or xenocrysts are reported from the area separating the Klamath Mountains Province and the Basin and Range. Though direct constraints are lacking, seismic data suggest that southern Cascade Range and Modoc Plateau crust are likely underlain by igneous and metamorphic rocks related to the Klamath Mountains Province and northern Sierra Nevada (e.g., Fuis et al., 1987).

6. CONCLUSIONS

The purpose of this effort is to constrain the origin of the CMS. To that end, new zircon U-Pb geochronology from the outer CMS unit points to ca. 171 Ma

eruption of volcanic protoliths and deposition of infolded, nonconformably overlying metasedimentary rocks shortly thereafter. Outer CMS sedimentary protoliths comprise chiefly Klamath Mountains Province-derived detritus. The greenschist–amphibolite grade inverted metamorphic field gradient preserved in the outer CMS is inferred to have formed during ca. 156–152 Ma underthrusting of the unit directly beneath the ca. 167–156 Ma (i.e., recently extinguished at that time and hence, hot) Wooley Creek plutonic belt. In aggregate, the outer CMS appears to represent products of early-stage Josephine basin rifting, akin to similar "rift edge facies" assemblages such as the China Peak and Preston Peak complexes, which underthrusted the Middle–Late Jurassic arc and its Rattlesnake Creek terrane framework during the Nevadan orogeny.

The inner CMS is petrogenetically distinct from the outer CMS to the degree that referring to each as portions of the same unit may no longer be practical. Detrital zircon U-Pb ages derived from the inner CMS reveal a down-section decrease in calculated MDAs from ca. 160 Ma adjacent to the Condrey internal fault to ca. 130 Ma at the deepest level of exposure. This observation, integrated with sparse K-Ar white mica age constraints, leads us to subdivide the inner CMS into structurally high- and low-White Mountain and Dry Lake subunits, respectively. Based on similar rock types and comparable detrital zircon age spectra, we correlate both subunits of the inner CMS with the eastern belt of the Franciscan Complex.

Tectonic underplating of the White Mountain subunit beneath previously emplaced outer CMS must predate the arrival of the Dry Lake subunit, to explain their older-on-younger structural arrangement (the former yields MDAs >10 m.y. older than the latter). The precise timing of underthrusting of each unit is unclear. However, we suspect that the White Mountain subunit was emplaced during the waning stages of the Nevadan event. Arrival of the Dry Lake subunit must postdate calculated MDAs spanning 143–130 Ma and possibly occurred at ca. 128 Ma, based on the K-Ar age of metamorphic white mica derived from this subunit.

These results suggest that the CMS represents forearc-trench assemblages emplaced beneath the Late Jurassic arc in at least three distinct pulses. The first two occurred in rapid succession, with underplating of the outer CMS and White Mountain subunit of the inner CMS taking place sequentially during and following the Nevadan event. Emplacement of the outer CMS, and possibly the White Mountain inner CMS subunit, involved significant tectonic erosion as evidenced by the rootless aspect of upper-plate plutons. Emplacement of the Dry Lake inner CMS subunit probably occurred some 10–20 m.y. later. The absence of Josephine ophiolite and its Galice Formation cover from the inner CMS point to removal of these lithologies during underthrusting.

The far inboard position of these assemblages requires shallow-angle thrust emplacement, which we attribute to shallow-angle subduction. We further argue that the spatial restriction of the Nevadan event to the Klamath Mountains Province plus northern Sierra Nevada, including deformation of the Josephine ophiolite but not the Coast Range ophiolite, is related to a relatively narrow (a few hundred kilometers) corridor of shallow-angle subduction that must have been periodic to allow for sequential underplating of the outer CMS and both subunits of the inner CMS. In particular, the >10 m.y. gap separating underplating of the White Mountain and Dry Lake subunits of the inner CMS, during which regional magmatism reignited before shutting down permanently when the Dry Lake subunit was emplaced, requires a phase of steeper subduction separating more shallowly dipping intervals. The tectonic scenario in which episodic shallow-angle subduction took place is unclear, though it may have been related to collision of separate thickened tracts of oceanic lithosphere ("tectonic switching" of Collins, 2002), buckling of the downgoing slab along mantle-density interfaces (e.g., Schellart and Strak, 2021), or perhaps a combination of the two.

Shallow-angle emplacement of the CMS had profound effects on the Klamath Mountains Province and adjacent geologic provinces in Late Jurassic and Early Cretaceous time. First, arc productivity waned during emplacement of the outer CMS and the White Mountain inner CMS subunit before shutting off entirely with the arrival of the Dry Lake subunit. Immediately following emplacement of the Dry Lake subunit, the entire Klamath Mountains Province separated from the Sierran arc and was translated ~200 km to the west into the forearc. Westward displacement of the Klamath Mountains Province coincided with regional cooling, low-angle normal faulting, and increasing sedimentation in the Great Valley forearc basin. We attribute these profound changes to rollback of the downgoing slab to a steeper trajectory, reducing interplate coupling and facilitating trenchward displacement of the entire Klamath Mountains Province.

The parallels between Late Jurassic to Early Cretaceous tectonism recorded by the Klamath Mountains Province and Late Cretaceous–early Cenozoic events of Southern California are striking. In each location, the upper-plate domain transitions from a phase of stable arc magmatism; then yields to diminishing magmatism, upper–mid-crustal shortening, and basal crustal tectonic erosion plus underplating; and culminates with extensional collapse. These relations are inferred, in each location, to have resulted from a transition from relatively steeply dipping to shallow-angle subduction and a return to a steeper dip. For the case of the Klamath Mountains Province, at least three such tectonic switching events are inferred. Recognition of similar sequences of events in the geologic record may aid in the identification of additional ancient examples of shallow-angle subduction damage zones and improve our understanding of how modern "snapshots" of shallow-angle subduction zones may evolve.

ACKNOWLEDGMENTS

This paper is dedicated to the memory of J. Saleeby (1948–2023) and J.D. Yule (1961–2022), to whom we are grateful for sharing their deep knowledge of Klamath geology. They are greatly missed. This effort benefitted from field and lab assistance by J. Anderson, A. Bleeker, R. Ceesay, J. Coons, R. DiCarlo, N. Sponseller, and K. Taylor, and discussions with C. Barnes, W. Behr, T. Dumitru, W.G. Ernst, K. Gates, B. Hacker, G. Harper, M. Helper, C. Jacobson, J. MacDonald, K. Surpless, and C. Tewksbury-Christle. The manuscript was greatly improved through thoughtful reviews by A. Yoshinobu and K. Surpless. This work was supported by National Science Foundation grant EAR-1846811 (to A.D. Chapman). The Siskiyou Field Institute is thanked for providing a base of operations for fieldwork.

REFERENCES CITED

Alberts, D., Gehrels, G.E., and Nelson, J., 2021, U-Pb and Hf analyses of detrital zircons from Paleozoic and Cretaceous strata on Vancouver Island, British Columbia: Constraints on the Paleozoic tectonic evolution of southern Wrangellia: Lithosphere, v. 2021, https://doi.org/10.2113/2021/7866944.

Allen, C.M., and Barnes, C.G., 2006, Ages and some cryptic sources of Mesozoic plutonic rocks in the Klamath Mountains, California and Oregon, *in* Snoke, A.W., and Barnes, C.G., eds., Geological Studies in the Klamath Mountains Province, California and Oregon: A Volume in Honor of William P. Irwin: Geological Society of America Special Paper 410, p. 223–245, https://doi.org/10.1130/2006.2410(11).

Arndt, N.T., 2013, The formation and evolution of the continental crust: Geochemical Perspectives, v. 2, no. 3, p. 405–533, https://doi.org/10.7185/geochempersp.2.3.

Barnes, C.G., and Barnes, M.A., 2020, The western Hayfork terrane: Remnants of the Middle Jurassic arc in the Klamath Mountain province, California and Oregon: Geosphere, v. 16, no. 4, p. 1058–1081, https://doi.org/10.1130/GES02229.1.

Barnes, C.G., Petersen, S.W., Kistler, R.W., Prestvik, T., and Sundvoll, B., 1992, Tectonic implications of isotopic variation among Jurassic and Early Cretaceous plutons, Klamath Mountains: Geological Society of America Bulletin, v. 104, p. 117–126, https://doi.org/10.1130/0016-7606(1992)104<0117:TIOIVA>2.3.CO;2.

Barnes, C.G., Petersen, S.W., Kistler, R.W., Murray, R., and Kays, M.A., 1996, Source and tectonic implications of tonalite-trondhjemite magmatism in the Klamath Mountains: Contributions to Mineralogy and Petrology, v. 123, p. 40–60, https://doi.org/10.1007/s004100050142.

Barnes, C.G., Mars, E.V., Swapp, S., and Frost, C.D., 2006, Petrology and geochemistry of the Middle Jurassic Ironside Mountain batholith: Evolution of potassic magmas in a primitive arc setting, *in* Snoke, A.W., and Barnes, C.G., eds., Geological Studies in the Klamath Mountains Province, California and Oregon: A Volume in Honor of William P. Irwin: Geological Society of America Special Paper 410, p. 199–221, https://doi.org/10.1130/2006.2410(10).

Barrow, W.M., and Metcalf, R.V., 2006, A reevaluation of the paleotectonic significance of the Paleozoic Central Metamorphic terrane, eastern Klamath Mountains, California: New constraints from trace element geochemistry and $^{40}Ar/^{39}Ar$ thermochronology, *in* Snoke, A.W., and Barnes, C.G., eds., Geological Studies in the Klamath Mountains Province, California and Oregon: A Volume in Honor of William P. Irwin: Geological Society of America Special Paper 410, p. 393–410, https://doi.org/10.1130/2006.2410(19).

Barrows, A.G., 1969, Geology of the Hamburg-McGuffy Creek area Siskiyou County, California, and petrology of the Tom Martin ultramafic complex [Ph.D. thesis]: Los Angeles, University of California, 301 p.

Batt, G.E., Harper, G.D., Heizler, M., and Roden-Tice, M., 2010a, Cretaceous sedimentary blanketing and tectonic rejuvenation in the western Klamath Mountains: Insights from thermochronology: Central European Journal of Geosciences, v. 2, p. 138–151.

Batt, G.E., Casman, S.M., Garver, J., and Bigelow, J.J., 2010b, Thermotectonic evidence for the consequences of two-stage extension on the Trinity detachment surface, Eastern Klamath Mountains: American Journal of Science, v. 310, p. 261–281, https://doi.org/10.2475/04.2010.02.

Berge, P.A., and Stauber, D.A., 1987, Seismic refraction study of upper crustal structure in the Lassen Peak Area, northern California: Journal of Geophysical Research: Solid Earth, v. 92, p. 10,571–10,579, https://doi.org/10.1029/JB092iB10p10571.

Berkland, J.O., Raymond, L.A., Kramer, J.C., Moores, E.M., and O'Day, M., 1972, What is Franciscan?: AAPG Bulletin, v. 56, p. 2295–2302.

Bird, P., 1979, Continental delamination and the Colorado Plateau: Journal of Geophysical Research: Solid Earth, v. 84, p. 7561–7571, https://doi.org/10.1029/JB084iB13p07561.

Black, L., Kamo, S.L., Allen, C.M., Davis, D.W., Aleinikoff, J.N., Valley, J.W., Mundil, M., Campbell, I.H., Korsch, R.J., Williams, I.S., and Foudoulis, C., 2004, Improved $^{206}Pb/^{238}U$ microprobe geochronology by the monitoring of a trace-element-related matrix effect; SHRIMP, ID-TIMS, ELA-ICP-MS and oxygen isotope documentation for a series of zircon standards: Chemical Geology, v. 205, p. 115–140, https://doi.org/10.1016/j.chemgeo.2004.01.003.

Blake, M.C., Jr., Engebretson, D.C., Jayko, A.S., and Jones, D.L., 1985, Tectonostratigraphic terranes in southwest Oregon, *in* Howell, D.G., ed., Tectonostratigraphic Terranes of the Circum-Pacific Region: Houston, Circum-Pacific Council for Energy and Mineral Resources, Earth Sciences Series 1, p. 147–157.

Blakey, R.C., and Ranney, W.D., 2018, Ancient Landscapes of Western North America: Cham, Switzerland, Springer, 228 p., https://doi.org/10.1007/978-3-319-59636-5.

Brown, E.H., and Blake, M.C., Jr., 1987, Correlation of Early Cretaceous blueschists in Washington, Oregon and northern California: Tectonics, v. 6, no. 6, p. 795–806, https://doi.org/10.1029/TC006i006p00795.

Brun, J.P., and Faccenna, C., 2008, Exhumation of high-pressure rocks driven by slab rollback: Earth and Planetary Science Letters, v. 272, p. 1–7, https://doi.org/10.1016/j.epsl.2008.02.038.

Burchfiel, B.C., Cowan, D.S., and Davis, G.A., 1992, Tectonic overview of the Cordilleran orogen in the western United States, *in* Burchfiel, B.C., Lipman, P.W., and Zoback, M.L., eds., The Cordilleran Orogen: Conterminous U.S.: Boulder, Colorado, Geological Society of America, Geology of North America, v. G3, p. 407–414, https://doi.org/10.1130/DNAG-GNA-G3.407.

Burton, W.C., 1982, Geology of the Scott Bar Mountains, northern California [M.S. thesis]: Eugene, University of Oregon, 120 p.

Cashman, S.M., and Elder, D.R., 2002, Post-Nevadan detachment faulting in the Klamath Mountains, California: Geological Society of America Bulletin, v. 114, p. 1520–1534, https://doi.org/10.1130/0016-7606(2002)114<1520:PNDFIT>2.0.CO;2.

Chapman, A.D., 2017, The Pelona–Orocopia–Rand and related schists of southern California: A review of the best-known archive of shallow subduction on the planet: International Geology Review, v. 59, no. 5–6, p. 664–701, https://doi.org/10.1080/00206814.2016.1230836.

Chapman, A.D., Yule, J.D., LaMaskin, T., and Schwartz, W., 2021b, Middle Jurassic to Early Cretaceous tectonic evolution of the western Klamath Mountains and outboard Franciscan assemblages, northern California-southern Oregon, USA, *in* Booth, A.M., and Grunder, A.L., eds., From Terranes to Terrains: Geologic Field Guides on the Construction and Destruction of the Pacific Northwest: Geological Society of America Field Guide 62, p. 73–130, https://doi.org/10.1130/2021.0062(04).

Chapman, J.B., Shields, J.E., Ducea, M.N., Paterson, S.R., Attia, S., and Ardill, K.E., 2021a, The causes of continental arc flare ups and drivers of episodic magmatic activity in Cordilleran orogenic systems: Lithos, v. 398–399, https://doi.org/10.1016/j.lithos.2021.106307.

Chen, J.H., and Moore, J.G., 1982, Uranium-lead isotopic ages from the Sierra Nevada batholith, California: Journal of Geophysical Research: Solid Earth, v. 87, p. 4761–4784, https://doi.org/10.1029/JB087iB06p04761.

Clift, P., and Vannucchi, P., 2004, Controls on tectonic accretion versus erosion in subduction zones: Implications for the origin and recycling of the continental crust: Reviews of Geophysics, v. 42, https://doi.org/10.1029/2003RG000127.

Cloos, M., and Shreve, R.L., 1988, Subduction-channel model of prism accretion, melange formation, sediment subduction, and subduction erosion at convergent plate margins: 1. Background and description: Pure and Applied Geophysics, v. 128, p. 455–500, https://doi.org/10.1007/BF00874548.

Coint, N., Barnes, C.G., Yoshinobu, A.S., Chamberlain, K.R., and Barnes, M.A., 2013, Batch-wise assembly and zoning of a tilted calc-alkaline batholith: Field relations, timing, and compositional variation: Geosphere, v. 9, p. 1729–1746, https://doi.org/10.1130/GES00930.1.

Coleman, R.G., Manning, C.E., Mortimer, N., Donato, M.M., and Hill, L.B., 1988, Tectonic and regional metamorphic framework of the Klamath Mountains and adjacent Coast Ranges, California and Oregon, *in* Ernst, W.G., ed., Metamorphism and Crustal Evolution of the Western United States—Rubey Volume VII: Englewood Cliffs, New Jersey, Prentice Hall, p. 1059–1097.

Collins, W.J., 2002, Hot orogens, tectonic switching, and creation of continental crust: Geology, v. 30, p. 535–538, https://doi.org/10.1130/0091-7613(2002)030<0535:HOTSAC>2.0.CO;2.

Coney, P.J., and Reynolds, S.J., 1977, Cordilleran Benioff zones: Nature, v. 270, p. 403–406, https://doi.org/10.1038/270403a0.

Constenius, K.N., Johnson, R.A., Dickinson, W.R., and Williams, T.A., 2000, Tectonic evolution of the Jurassic-Cretaceous Great Valley forearc, California: Implications for the Franciscan thrust-wedge hypothesis: Geological Society of America Bulletin, v. 112, p. 1703–1723, https://doi.org/10.1130/0016-7606(2000)112<1703:TEOTJC>2.0.CO;2.

Cornwall, H.R., 1981, Chromite deposits in the Seiad Valley and Scott Bar quadrangles, Siskiyou County, California: U.S. Geological Survey Bulletin 1382-D, p. DI–D17.

Coutts, D.S., Matthews, W.A., and Hubbard, S.M., 2019, Assessment of widely used methods to derive depositional ages from detrital zircon populations: Geoscience Frontiers, v. 10, no. 4, p. 1421–1435, https://doi.org/10.1016/j.gsf.2018.11.002.

Darby, B.J., Wyld, S.J., and Gehrels, G.E., 2000, Provenance and paleogeography of the Black Rock terrane, northwestern Nevada, *in* Soreghan, M.J., and Gehrels, G.E., eds., Paleozoic and Triassic Paleogeography and Tectonics of Western Nevada and Northern California: Geological Society of America Special Paper 347, p. 77–88, https://doi.org/10.1130/0-8137-2347-7.77.

Davies, J.H., and Stevenson, D.J., 1992, Physical model of source region of subduction zone volcanics: Journal of Geophysical Research: Solid Earth, v. 97, p. 2037–2070, https://doi.org/10.1029/91JB02571.
Davis, G.A., 1968, Westward thrust faulting in the south-central Klamath Mountains, California: Geological Society of America Bulletin, v. 79, p. 911–934, https://doi.org/10.1130/0016-7606(1968)79[911:WTFITS]2.0.CO;2.
de Capitani, C., and Brown, T.H., 1987, The computation of chemical equilibria in complex systems containing non-ideal solutions: Geochimica et Cosmochimica Acta, v. 51, p. 2639–2652, https://doi.org/10.1016/0016-7037(87)90145-1.
DeGraaff-Surpless, K., Graham, S.A., Wooden, J.L., and McWilliams, M.O., 2002, Detrital zircon provenance analysis of the Great Valley Group, California: Evolution of an arc-forearc system: Geological Society of America Bulletin, v. 114, p. 1564–1580, https://doi.org/10.1130/0016-7606(2002)114<1564:DZPAOT>2.0.CO;2.
Dewey, J.F., 1981, Episodicity, sequence and style at convergent plate boundaries: The Continental Crust and Its Mineral Deposits, *in* Strangeway, D.W., ed., The Continental Crust and its Mineral Deposits: Geological Association of Canada Special Paper 20, p. 553–572.
Dickinson, W.R., 2000, Geodynamic interpretation of Paleozoic tectonic trends oriented oblique to the Mesozoic Klamath-Sierran continental margin in California, *in* Soreghan, M.J., and Gehrels, G.E., eds., Paleozoic and Triassic Paleogeography and Tectonics of Western Nevada and Northern California: Geological Society of America Special Paper 347, p. 209–245, https://doi.org/10.1130/0-8137-2347-7.209.
Dickinson, W.R., 2004, Evolution of the North American Cordillera: Annual Review of Earth and Planetary Sciences, v. 32, p. 13–45, https://doi.org/10.1146/annurev.earth.32.101802.120257.
Dickinson, W.R., and Gehrels, G.E., 2003, U-Pb ages of detrital zircons from Permian and Jurassic eolian sandstones of the Colorado Plateau, USA: Paleogeographic implications: Sedimentary Geology, v. 163, p. 29–66, https://doi.org/10.1016/S0037-0738(03)00158-1.
Dickinson, W.R., and Gehrels, G.E., 2008, U-Pb ages of detrital zircons in Jurassic eolian and associated sandstones of the Colorado Plateau: Evidence for transcontinental dispersal and intraregional recycling of sediment: Geological Society of America Bulletin, v. 121, p. 408–433, https://doi.org/10.1130/B26406.1.
Dickinson, W.R., and Gehrels, G.E., 2009, Use of U-Pb ages of detrital zircons to infer maximum depositional ages of strata: A test against a Colorado Plateau Mesozoic database: Earth and Planetary Science Letters, v. 288, p. 115–125, https://doi.org/10.1016/j.epsl.2009.09.013.
Donato, M.M., 1987, Evolution of an ophiolitic tectonic mélange, Marble Mountains, northern California Klamath Mountains: Geological Society of America Bulletin, v. 98, p. 448–464, https://doi.org/10.1130/0016-7606(1987)98<448:EOAOTM>2.0.CO;2.
Donato, M.M., Barnes, C.G., and Tomlinson, S.L., 1996, The enigmatic Applegate Group of southwestern Oregon: Age, correlation, and tectonic affinity: Oregon Geology, v. 58, p. 79–91.
Ducea, M.N., Kidder, S., Chesley, J.T., and Saleeby, J., 2009, Tectonic underplating of trench sediments beneath magmatic arcs: The central California example: International Geology Review, v. 51, no. 1, p. 1–26, https://doi.org/10.1080/00206810802602767.
Dumitru, T.A., Wright, J.E., Wakabayashi, J., and Wooden, J.L., 2010, Early Cretaceous transition from nonaccretionary behavior to strongly accretionary behavior within the Franciscan subduction complex: Tectonics, v. 29, TC5001, https://doi.org/10.1029/2009TC002542.
Engebretson, D.C., Cox, A., and Thompson, G.A., 1984, Correlation of plate motions with continental tectonics: Laramide to Basin-Range: Tectonics, v. 3, no. 2, p. 115–119, https://doi.org/10.1029/TC003i002p00115.
Ernst, W.G., 1990, Accretionary terrane in the Sawyers Bar area of the Western Triassic and Paleozoic Belt, central Klamath Mountains, northern California, *in* Harwood, D.S., and Miller, M.M., eds., Paleozoic and Early Mesozoic Paleogeographic Relations: Sierra Nevada, Klamath Mountains, and Related Terranes: Geological Society of America Special Paper 225, p. 297–306, https://doi.org/10.1130/SPE255-p297.
Ernst, W.G., 2013, Earliest Cretaceous Pacificward offset of the Klamath Mountains salient, NW California–SW Oregon: Lithosphere, v. 5, p. 151–159, https://doi.org/10.1130/L247.1.
Ernst, W.G., 2017, Geologic evolution of a Cretaceous tectonometamorphic unit in the Franciscan Complex, western California: International Geology Review, v. 59, no. 5–6, p. 563–576, https://doi.org/10.1080/00206814.2016.1201440.
Ernst, W.G., Wu, C., Lai, M., and Zhang, X., 2017, U-Pb ages and sedimentary provenance of detrital zircons from eastern Hayfork meta-argillites, Sawyers Bar area, northwestern California: The Journal of Geology, v. 125, p. 33–44, https://doi.org/10.1086/689186.
Evarts, R.C., and Schiffman, P., 1983, Submarine hydrothermal metamorphism of the Del Puerto ophiolite, California: American Journal of Science, v. 283, p. 289–340, https://doi.org/10.2475/ajs.283.4.289.
Ferrari, L., Orozco-Esquivel, T., Manea, V., and Manea, M., 2012, The dynamic history of the Trans-Mexican Volcanic Belt and the Mexico subduction zone: Tectonophysics, v. 522, p. 122–149, https://doi.org/10.1016/j.tecto.2011.09.018.
Fuis, G.S., Zucca, J.J., Mooney, W.D., and Milkereit, B., 1987, A geologic interpretation of seismic-refraction results in northeastern California: Geological Society of America Bulletin, v. 98, p. 53–65, https://doi.org/10.1130/0016-7606(1987)98<53:AGIOSR>2.0.CO;2.
Garlick, S.R., Medaris, L.G., Jr., Snoke, A.W., Schwartz, J.J., and Swapp, S.M., 2009, Granulite- to amphibolite-facies metamorphism and penetrative deformation in a disrupted ophiolite, Klamath Mountains, California: A deep view into the basement of an accreted oceanic arc, *in* Miller, R.B., and Snoke, A.W., eds., Crustal Cross Sections from the Western North American Cordillera and Elsewhere: Implications for Tectonic and Petrologic Processes: Geological Society of America Special Paper 456, p. 151–186, https://doi.org/10.1130/2009.2456(06).
Gates, K., Yoshinobu, A., Barnes, C.G., Dailey, S.R., and Leib, S., 2019, Inverted metamorphic gradients and cryptic contacts surrounding the enigmatic Condrey Mountain dome, Klamath Mountain province, CA and OR: Geological Society of America Abstracts with Programs, v. 51, no. 4, https://doi.org/10.1130/abs/2019CD-329660.
Gehrels, G., Valencia, V., and Pullen, A., 2006, Detrital zircon geochronology by laser-ablation multicollector ICPMS at the Arizona Laserchron Center: The Paleontological Society Papers, v. 12, p. 67–76, https://doi.org/10.1017/S1089332600001352.
Gehrels, G., Valencia, V.A., and Ruiz, J., 2008, Enhanced precision, accuracy, efficiency, and spatial resolution of U-Pb ages by laser ablation–multicollector–inductively coupled plasma–mass spectrometry: Geochemistry, Geophysics, Geosystems, v. 9, no. 3, https://doi.org/10.1029/2007GC001805.
Gehrels, G.E., and Miller, M.M., 2000, Detrital zircon geochronologic study of Upper Paleozoic strata in the eastern Klamath terrane, northern California, *in* Soreghan, M.J., and Gehrels, G.E., eds., Paleozoic and Triassic Paleogeography and Tectonics of Western Nevada and Northern California: Geological Society of America Special Paper 347, p. 99–108, https://doi.org/10.1130/0-8137-2347-7.99.
Gehrels, G.E., and Pecha, M., 2014, Detrital zircon U-Pb geochronology and Hf isotope geochemistry of Paleozoic and Triassic passive margin strata of western North America: Geosphere, v. 10, p. 49–65, https://doi.org/10.1130/GES00889.1.
Goodge, J.W., 1989, Polyphase metamorphic evolution of a Late Triassic subduction complex, Klamath Mountains, northern California: American Journal of Science, v. 289, p. 874–943, https://doi.org/10.2475/ajs.289.7.874.
Gradstein, F.M., Ogg, J.G., Schmitz, M.D., and Ogg, G.M., 2020, The Geologic Time Scale 2020: Amsterdam, Netherlands, Elsevier, 1357 p.
Grove, M., Jacobson, C.E., Barth, A.P., and Vucic, A., 2003, Temporal and spatial trends of Late Cretaceous–Early Tertiary underplating of Pelona and related schist beneath southern California and southwestern Arizona, *in* Johnson, S.E., Patterson, S.R., Fletcher, J.M., Girty, G.H., Kimbrough, D.L., and Martin-Barajas, A., eds., Tectonic Evolution of Northwestern Mexico and the Southwestern USA: Geological Society of America Special Paper 374, p. 381–406, https://doi.org/10.1130/0-8137-2374-4.381.
Grove, M., Gehrels, G.E., Cotkin, S.J., Wright, J.E., and Zou, H., 2008, Non-Laurentian cratonal provenance of Late Ordovician eastern Klamath blueschists and a link to the Alexander terrane, *in* Wright, J.E., and Shervais, J.W., eds., Ophiolites, Arcs, and Batholiths: A Tribute to Cliff Hopson: Geological Society of America Special Paper 438, p. 223–250, https://doi.org/10.1130/2008.2438(08).
Guffanti, M., Clynne, M.A., and Muffler, L.J.P., 1996, Thermal and mass implications of magmatic evolution in the Lassen volcanic region, California, and minimum constraints on basalt influx to the lower crust: Journal of Geophysical Research: Solid Earth, v. 101, p. 3003–3013, https://doi.org/10.1029/95JB03463.
Gutscher, M.A., Spakman, W., Bijwaard, H., and Engdahl, E.R., 2000, Geodynamics of flat subduction: Seismicity and tomographic constraints from the Andean margin: Tectonics, v. 19, p. 814–833, https://doi.org/10.1029/1999TC001152.
Hacker, B., and Ernst, W.G., 1993, Jurassic orogeny in the Klamath Mountains: A geochronological analysis, *in* Dunne, G., and McDougall, K., eds., Mesozoic Paleogeography of the Western United States–II: SEPM (Society for Sedimentary Geology) Book 71, Pacific Section, p. 37–60.
Hacker, B.R., Donato, M.M., Barnes, C.G., McWilliams, M.O., and Ernst, W.G., 1995, Timescales of orogeny: Jurassic construction of the Klamath Mountains: Tectonics, v. 14, p. 677–703, https://doi.org/10.1029/94TC02454.
Hacker, B.R., Kelemen, P.B., and Behn, M.D., 2011, Differentiation of the continental crust by relamination: Earth and Planetary Science Letters, v. 307, p. 501–516, https://doi.org/10.1016/j.epsl.2011.05.024.

Harper, G.D., 1984, The Josephine ophiolite: Geological Society of America Bulletin, v. 95, p. 1009–1026, https://doi.org/10.1130/0016-7606(1984)95<1009:TJONC>2.0.CO;2.

Harper, G.D., 2003, Fe-Ti basalts and propagating rift tectonics in the Josephine ophiolite: Geological Society of America Bulletin, v. 115, p. 771–787, https://doi.org/10.1130/0016-7606(2003)115<0771:FBAPTI>2.0.CO;2.

Harper, G.D., and Wright, J.E., 1984, Middle to Late Jurassic tectonic evolution of the Klamath Mountains, California-Oregon: Tectonics, v. 3, p. 759–772, https://doi.org/10.1029/TC003i007p00759.

Harper, G.D., Saleeby, J.B., and Heizler, M., 1994, Formation and emplacement of the Josephine ophiolite, and the age of the Nevadan orogeny in the Klamath Mountains, California-Oregon: U/Pb zircon and $^{40}Ar/^{39}Ar$ geochronology: Journal of Geophysical Research: Solid Earth, v. 99, p. 4293–4321, https://doi.org/10.1029/93JB02061.

Helper, M., 1985, Structural, metamorphic and geochronologic constraints on the origin of the Condrey Mountain Schist, north central Klamath Mountains, northern California [Ph.D. dissertation]: Austin, Texas, University of Texas at Austin, 209 p.

Helper, M.A., 1986, Deformation and high P/T metamorphism in the central part of the Condrey Mountain window, north-central Klamath Mountains, California and Oregon, *in* Evans, B.W., and Brown, E.H., eds., Blueschists and Eclogites: Geological Society of America Memoir 164, p. 125–142, https://doi.org/10.1130/MEM164-p125.

Hill, L.B., 1984, A tectonic and metamorphic history of the north-central Klamath Mountains, California [Ph.D. thesis]: Stanford, California, Stanford University, 248 p.

Hotz, P.E., 1979, Regional metamorphism in the Condrey Mountain quadrangle, north-central Klamath Mountains, California: U.S. Geological Survey Professional Paper 1086, 25 p., https://doi.org/10.3133/pp1086.

Hotz, P.E., Lanphere, M.A., and Swanson, D.A., 1977, Triassic blueschist from northern California and north-central Oregon: Geology, v. 5, p. 659–663, https://doi.org/10.1130/0091-7613(1977)5<659:TBFNCA>2.0.CO;2.

Irwin, W.P., 1960, Geologic reconnaissance of the northern Coast Ranges and Klamath Mountains, California, with a summary of the mineral resources: San Francisco, California Division of Mines Bulletin 179, 80 p.

Irwin, W.P., 1972, Terranes of the western Paleozoic and Triassic belt in the southern Klamath Mountains, California, *in* Geological Survey Research 1972, Chapter C: U.S. Geological Survey Professional Paper 800-C, p. C103–C111.

Irwin, W.P., 2003, Correlation of the Klamath Mountains and Sierra Nevada: U.S. Geological Survey Open-File Report 02–490, 2 map sheets, https://pubs.usgs.gov/of/2002/0490/.

Irwin, W.P., and Wooden, J.L., 1999, Plutons and accretionary episodes of the Klamath Mountains, California and Oregon: U.S. Geological Survey Open-File Report 99–0374, 1 sheet.

Jacobson, C.E., Grove, M., Vucic, A., Pedrick, J.N., and Ebert, K.A., 2007, Exhumation of the Orocopia Schist and associated rocks of southeastern California: Relative roles of erosion, synsubduction tectonic denudation, and middle Cenozoic extension, *in* Cloos, M., Carlson, W.D., Gilbert, M.C., Liou, J.G., and Sorensen, S.S., Convergent Margin Terranes and Associated Regions: A Tribute to W.G. Ernst: Geological Society of America Special Paper 419, p. 1–37, https://doi.org/10.1130/2007.2419(01).

Jacobson, C.E., Grove, M., Pedrick, J.N., Barth, A.P., Marsaglia, K.M., Gehrels, G.E., and Nourse, J.A., 2011, Late Cretaceous–early Cenozoic tectonic evolution of the southern California margin inferred from provenance of trench and forearc sediments: Geological Society of America Bulletin, v. 123, no. 3–4, p. 485–506, https://doi.org/10.1130/B30238.1.

Johnston, S.T., and Borel, G.D., 2007, The odyssey of the Cache Creek terrane, Canadian Cordillera: Implications for accretionary orogens, tectonic setting of Panthalassa, the Pacific superwell, and break-up of Pangea: Earth and Planetary Science Letters, v. 253, p. 415–428, https://doi.org/10.1016/j.epsl.2006.11.002.

Jones, D.L., and Irwin, W.P., 1971, Structural implications of an offset Early Cretaceous shoreline in northern California: Geological Society of America Bulletin, v. 82, p. 815–822, https://doi.org/10.1130/0016-7606(1971)82[815:SIOAOE]2.0.CO;2.

Kay, R.W., and, Mahlburg-Kay, S., 1991, Creation and destruction of lower continental crust: Geologische Rundschau, v. 80, p. 259–278.

Klapper, M., and Chapman, A., 2017, Inverted metamorphism of the Condrey Mountain schist (northern California/southern Oregon): A ~30 myr record of subduction initiation and maturation beneath a cooling upper plate: Geological Society of America Abstracts with Programs, v. 49, no. 4, https://doi.org/10.1130/abs/2017CD-292952.

Klein, C.W., 1977, Thrust plates of the north-central Klamath Mountains near Happy Camp, California: California Division of Mines and Geology Special Report 129, p. 23–26.

Lallemand, S., Peyret, M., van Rijsingen, E., Arcay, D., and Heuret, A., 2018, Roughness characteristics of oceanic seafloor prior to subduction in relation to the seismogenic potential of subduction zones: Geochemistry, Geophysics, Geosystems, v. 19, no. 7, p. 2121–2146, https://doi.org/10.1029/2018GC007434.

LaMaskin, T.A., Vervoort, J.D., Dorsey, R.J., and Wright, J.E., 2011, Early Mesozoic paleogeography and tectonic evolution of the western United States: Insights from detrital zircon U-Pb geochronology, Blue Mountains Province, northeastern Oregon: Geological Society of America Bulletin, v. 123, p. 1939–1965, https://doi.org/10.1130/B30260.1.

LaMaskin, T.A., Rivas, J.A., Barbeau, D.L., Schwartz, J.J., Russell, J.A., and Chapman, A.D., 2021, A crucial geologic test of Late Jurassic exotic collision versus endemic re-accretion in the Klamath Mountains Province, western United States, with implications for the assembly of western North America: Geological Society of America Bulletin, v. 134, p. 965–988, https://doi.org/10.1130/B35981.1.

Lanphere, M.A., Irwin, W.P., and Hotz, P.E., 1968, Isotopic age of the Nevadan orogeny and older plutonic and metamorphic events in the Klamath Mountains, California: Geological Society of America Bulletin, v. 79, p. 1027–1052, https://doi.org/10.1130/0016-7606(1968)79[1027:IAOTNO]2.0.CO;2.

Liu, L., Gurnis, M., Seton, M., Saleeby, J., Müller, R.D., and Jackson, J., 2010, The role of oceanic plateau subduction in the Laramide orogeny: Nature Geoscience, v. 3, p. 353–357, https://doi.org/10.1038/ngeo829.

Ludwig, K.R., 2003, Mathematical-statistical treatment of data and errors for $^{230}Th/U$ geochronology: Reviews in Mineralogy and Geochemistry, v. 52, p. 631–656, https://doi.org/10.2113/0520631.

Lund, K., and Snee, L.W., 1988, Metamorphism, structural development, and age of the continent-island arc juncture in west-central Idaho, *in* Ernst, W.G., ed., Metamorphism and Crustal Evolution of the Western United States—Rubey Volume III: Englewood Cliffs, New Jersey, Prentice Hall, p. 297–331.

MacDonald, J.H., Jr., Harper, G.D., and Zhu, B., 2006, Petrology, geochemistry, and provenance of the Galice Formation, Klamath Mountains, Oregon and California, *in* Snoke, A.W., and Barnes, C.G., eds., Geological Studies in the Klamath Mountains Province, California and Oregon: A Volume in Honor of William P. Irwin: Geological Society of America Special Paper 410, p. 77–101, https://doi.org/10.1130/2006.2410(04).

Manuszak, J.D., Satterfield, J.I., and Gehrels, G.E., 2000, Detrital-zircon geochronology of Upper Triassic strata in western Nevada, *in* Soreghan, M.J., and Gehrels, G.E., eds., Paleozoic and Triassic Paleogeography and Tectonics of Western Nevada and Northern California: Geological Society of America Special Paper 347, p. 109–118, https://doi.org/10.1130/0-8137-2347-7.109.

Mauel, D.J., Lawton, T.F., González-León, C., Iriondo, A., and Amato, J.M., 2011, Stratigraphy and age of Upper Jurassic strata in north-central Sonora, Mexico: Southwestern Laurentian record of crustal extension and tectonic transition: Geosphere, v. 7, p. 390–414, https://doi.org/10.1130/GES00600.1.

May, S.R., and Butler, R.F., 1986, North American Jurassic apparent polar wonder: Implications for plate motion, paleogeography and Cordilleran tectonics: Journal of Geophysical Research: Solid Earth, v. 91, p. 11,519–11,544, https://doi.org/10.1029/JB091iB11p11519.

May, S.R., Beck, M.E., Jr., and Butler, R.F., 1989, North American apparent polar wander, plate motion, and left-oblique convergence: Late Jurassic–Early Cretaceous orogenic consequences: Tectonics, v. 8, p. 443–451, https://doi.org/10.1029/TC008i003p00443.

McClelland, W.C., Gehrels, G.E., and Saleeby, J.B., 1992, Upper Jurassic–Lower Cretaceous basinal strata along the Cordilleran margin: Implications for the accretionary history of the Alexander-Wrangellia-Peninsular terrane: Tectonics, v. 11, p. 823–835, https://doi.org/10.1029/92TC00241.

Medaris, L.G., Jr., 1966, Geology of the Seiad Valley area, Siskiyou County, California, and petrology of the Seiad ultramafic complex [Ph.D. thesis]: Los Angeles, University of California, Los Angeles, 333 p.

Miller, M.M., 1987, Dispersed remnants of a northeast Pacific fringing arc: Upper Paleozoic terranes of Permian McCloud faunal affinity, western U.S: Tectonics, v. 6, p. 807–830, https://doi.org/10.1029/TC006i006p00807.

Miller, M.M., and Saleeby, J.B., 1995, U-Pb geochronology of detrital zircon from Upper Jurassic synorogenic turbidites, Galice Formation, and related rocks, western Klamath Mountains: Correlation and Klamath Mountains provenance: Journal of Geophysical Research: Solid Earth, v. 100, p. 18,045–18,058, https://doi.org/10.1029/95JB00761.

Moores, E.M., 1970, Ultramafics and orogeny, with models of the US Cordillera and the Tethys: Nature, v. 228, p. 837–842, https://doi.org/10.1038/228837a0.

Mortimer, N., and Coleman, R.G., 1985, A Neogene structural dome in the Klamath Mountains, California: Geology, v. 13, p. 253–256, https://doi.org/10.1130/0091-7613(1985)13<253:ANSDIT>2.0.CO;2.

Orme, D.A., and Surpless, K.D., 2019, The birth of a forearc: The basal Great Valley Group, California, USA: Geology, v. 47, p. 757–761, https://doi.org/10.1130/G46283.1.

Paces, J.B., and Miller, J.D., 1993, Precise U-Pb ages of Duluth Complex and related mafic intrusions, northeastern Minnesota: Geochronological insights to physical, petrogenic, paleomagnetic, and tectonomagmatic processes associated with the 1.1 Ga Midcontinent Rift System: Journal of Geophysical Research: Solid Earth, v. 98, p. 13,997–14,013, https://doi.org/10.1029/93JB01159.

Pérez-Campos, X., Kim, Y., Husker, A., Davis, P.M., Clayton, R.W., Iglesias, A., Pacheco, J.F., Singh, S.K., Manea, V.C., and Gurnis, M., 2008, Horizontal subduction and truncation of the Cocos Plate beneath central Mexico: Geophysical Research Letters, v. 35, https://doi.org/10.1029/2008GL035127.

Saleeby, J., 2003, Segmentation of the Laramide slab—Evidence from the southern Sierra Nevada region: Geological Society of America Bulletin, v. 115, p. 655–668, https://doi.org/10.1130/0016-7606(2003)115%3C0655:SOTLSF%3E2.0.CO;2.

Saleeby, J., 2007, The western extent of the Sierra Nevada batholith in the Great Valley basement and its significance in underlying mantle dynamics: Abstract T31E–02 presented at 2007 Fall Meeting, AGU, San Francisco, California, 10–14 December.

Saleeby, J.B., and Harper, G.D., 1993, Tectonic relations between the Galice Formation and the schists of Condrey Mountain, Klamath Mountains, northern California, *in* Dunne, G., and McDougall, K., eds., Mesozoic Paleography of the Western United States–II: SEPM (Society for Sedimentary Geology) Book 71, Pacific Section, p. 61–80.

Saleeby, J.B., Harper, G.D., Snoke, A.W., and Sharp, W.D., 1982, Time relations and structural-stratigraphic patterns in ophiolite accretion, west central Klamath Mountains, California: Journal of Geophysical Research: Solid Earth, v. 87, p. 3831–3848, https://doi.org/10.1029/JB087iB05p03831.

Schellart, W.P., and Strak, V., 2021, Geodynamic models of short lived, long-lived and periodic flat slab subduction: Geophysical Journal International, v. 226, p. 1517–1541, https://doi.org/10.1093/gji/ggab126.

Scherer, H.H., and Ernst, W.G., 2008, North Fork terrane, Klamath Mountains, California: Geologic, geochemical, and geochronologic evidence for an early Mesozoic forearc, *in* Wright, J.E., and Shervais, J.W., eds., Ophiolites, Arcs, and Batholiths: Geological Society of America Special Paper 438, p. 289–309, https://doi.org/10.1130/2008.2438(10).

Scherer, H.H., Ernst, W.G., and Wooden, J.L., 2010, Regional detrital zircon provenance of exotic metasandstone blocks, Eastern Hayfork terrane, western Paleozoic and Triassic belt, Klamath Mountains, California: The Journal of Geology, v. 118, p. 641–653, https://doi.org/10.1086/656352.

Scholl, D.W., and von Huene, R., 2007, Crustal recycling at modern subduction zones applied to the past: Issues of growth and preservation of continental basement crust, mantle geochemistry, and super-continent reconstruction, *in* Hatcher, Jr., R.D., et al., eds., 4-D Framework of Continental Crust: Geological Society of America Memoir 200, p. 9–32, https://doi.org/10.1130/MEM200.

Scholl, D.W., and von Huene, R., 2009, Implications of estimated magmatic additions and recycling losses at the subduction zones of accretionary (non-collisional) and collisional (suturing) orogens, *in* Cawood, P., and Kröner, A., eds., Accretionary Orogens in Space and Time: Geological Society, London, Special Publication 318, p. 105–125, https://doi.org/10.1144/SP318.4.

Schweickert, R.A., and Cowan, D.S., 1975, Early Mesozoic tectonic evolution of the western Sierra Nevada, California: Geological Society of America Bulletin, v. 86, p. 1329–1336, https://doi.org/10.1130/0016-7606(1975)86<1329:EMTEOT>2.0.CO;2.

Schweickert, R.A., Bogen, N.L., Girty, G.H., Hanson, R.E., and Merguerian, C., 1984, Timing and structural expression of the Nevadan orogeny, Sierra Nevada, California: Geological Society of America Bulletin, v. 95, p. 967–979, https://doi.org/10.1130/0016-7606(1984)95<967:TASEOT>2.0.CO;2.

Seton, M., Müller, R.D., Zahirovic, S., Gaina, C., Torsvik, T., Shephard, G., Talsma, A., Gurnis, M., Turner, M., and Chandler, M., 2012, Global continental and ocean basin reconstructions since 200 Ma: Earth-Science Reviews, v. 113, p. 212–270, https://doi.org/10.1016/j.earscirev.2012.03.002.

Sharman, G.R., Sharman, J.P., and Sylvester, Z., 2018, A Python-based toolset for visualizing and analyzing detrital geo-thermochronologic data: The Depositional Record: The Journal of the International Association of Sedimentologists, v. 4, p. 202–215, https://doi.org/10.1002/dep2.45.

Shervais, J.W., Kimbrough, D.L., Renne, P., Hanan, B.B., Murchey, B., Snow, C.A., Zoglman-Schuman, M.M., and Beaman, J., 2004, Multi-stage origin of the Coast Range ophiolite, California: Implications for the life cycle of supra-subduction zone ophiolites: International Geology Review, v. 46, p. 289–315, https://doi.org/10.2747/0020-6814.46.4.289.

Snoke, A.W., 1977, A thrust plate of ophiolitic rocks in the Preston Peak area, Klamath Mountains, California: Geological Society of America Bulletin, v. 88, p. 1641–1659, https://doi.org/10.1130/0016-7606(1977)88<1641:ATPOOR>2.0.CO;2.

Snoke, A.W., and Barnes, C.G., 2006, The development of tectonic concepts for the Klamath Mountains Province, California and Oregon, *in* Snoke, A.W., and Barnes, C.G., eds., Geological Studies in the Klamath Mountains Province, California and Oregon: A Volume in Honor of William P. Irwin: Geological Society of America Special Paper 410, p. 1–29, https://doi.org/10.1130/2006.2410(01).

Snow, C.A., Wakabayashi, J., Ernst, W.G., and Wooden, J.L., 2010, Detrital zircon evidence for progressive underthrusting in Franciscan metagraywackes, west-central California: Geological Society of America Bulletin, v. 122, p. 282–291, https://doi.org/10.1130/B26399.1.

Speed, R.C., 1977, Island-arc and other paleogeographic terranes of late Paleozoic age in the western Great Basin, *in* Stewart, J.H., Stevens, C.H., and Fritsche, A.E., eds., Paleozoic Paleogeography of the Western United States: Pacific Section, Society of Economic Paleontologists and Mineralogists, p. 349–362.

Speed, R.C., 1979, Collided Paleozoic microplate in the western U.S: The Journal of Geology, v. 87, p. 279–292, https://doi.org/10.1086/628417.

Stern, R.J., and Scholl, D.W., 2010, Yin and yang of continental crust creation and destruction by plate tectonic processes: International Geology Review, v. 52, p. 1–31, https://doi.org/10.1080/00206810903332322.

Suppe, J., and Armstrong, R.L., 1972, Potassium-argon dating of Franciscan metamorphic rocks: American Journal of Science, v. 272, no. 3, p. 217–233, https://doi.org/10.2475/ajs.272.3.217.

Surpless, K.D., Graham, S.A., Covault, J.A., and Wooden, J.L., 2006, Does the Great Valley Group contain Jurassic strata? Reevaluation of the age and early evolution of a classic forearc basin: Geology, v. 34, p. 21–24, https://doi.org/10.1130/G21940.1.

Surpless, K.D., Alford, R.W., Barnes, C., Yoshinobu, A. and Weis, N.E., 2024, Late Jurassic paleogeography of the US Cordillera from detrital zircon age and hafnium analysis of the Galice Formation, Klamath Mountains, Oregon and California, USA: Geological Society of America Bulletin, v. 136, p. 1488–1510, https://doi.org/10.1130/B36810.1.

Tewksbury-Christle, C.M., Behr, W.M., and Helper, M.A., 2021, Tracking deep sediment underplating in a fossil subduction margin: Implications for interface rheology and mass and volatile recycling: Geochemistry, Geophysics, Geosystems, v. 22, p. 1–23, https://doi.org/10.1029/2020GC009463.

Tewksbury-Christle, C.M., Behr, W.M., Helper, M.A., and Stockli, D.F., 2024, Tectonic evolution of the Condrey Mountain Schist: An intact record of Late Jurassic to Early Cretaceous Franciscan subduction and underplating: Tectonics, v. https://doi.org/10.1029/2023TC008115.

Tipper, H.W., 1984, The allochthonous Jurassic-Early Cretaceous terranes of the Canadian Cordillera and their relation to correlative strata of the North American craton, *in* Westermann, G.E.G., ed., Jurassic-Cretaceous Biochronology and Paleogeography of North America: Geological Association of Canada Special Paper 27, p. 113–120.

Underwood, M., Bachman, S.B., and Schweller, W.J., 1980, Sedimentary processes and facies associations within trench and trench-slope settings, *in* Field, M.E., et al., eds., Quaternary Depositional Environments on the Pacific Continental Margin: Pacific Coast Paleogeography Symposium 4: Society of Economic Paleontologists and Mineralogists, Pacific Section, p. 211–229.

U.S. Geological Survey, 1979, USGS 1:100000-scale Quadrangle for Yreka, CA 1979, https://ngmdb.usgs.gov/.

U.S. Geological Survey, 1983, USGS 1:100000-scale Quadrangle for Happy Camp, CA 1983, https://ngmdb.usgs.gov/.

Vermeesch, P., 2012, On the visualisation of detrital age distributions: Chemical Geology, v. 312–313, p. 190–194, https://doi.org/10.1016/j.chemgeo.2012.04.021.

Vermeesch, P., 2013, Multi-sample comparison of detrital age distributions: Chemical Geology, v. 341, p. 140–146, https://doi.org/10.1016/j.chemgeo.2013.01.010.

Vermeesch, P., 2021, Maximum depositional age estimation revisited: Geoscience Frontiers, v. 12, p. 843–850, https://doi.org/10.1016/j.gsf.2020.08.008.

von Huene, R., and Lallemand, S., 1990, Tectonic erosion along the Japan and Peru convergent margins: Geological Society of America Bulletin, v. 102, p. 704–720, https://doi.org/10.1130/0016-7606(1990)102<0704:TEATJA>2.3.CO;2.

von Huene, R., and Scholl, D.W., 1991, Observations at convergent margins concerning sediment subduction, subduction erosion, and the growth of continental crust: Reviews of Geophysics, v. 29, p. 279–316, https://doi.org/10.1029/91RG00969.

Wakabayashi, J., 2015, Anatomy of a subduction complex: Architecture of the Franciscan Complex, California, at multiple length and time scales: International Geology Review, v. 57, no. 5–8, p. 669–746, https://doi.org/10.1080/00206814.2014.998728.

Wallin, E.T., and Metcalf, R.V., 1998, Supra-subduction zone ophiolite formed in an extensional forearc: Trinity terrane, Klamath Mountains, California: The Journal of Geology, v. 106, p. 591–608, https://doi.org/10.1086/516044.

Wallin, E.T., Noto, R.C., and Gehrels, G.E., 2000, Provenance of the Antelope Mountain Quartzite, Yreka terrane, California: Evidence for large-scale late Paleozoic sinistral displacement along the North American Cordilleran margin and implications for the mid-Paleozoic fringing-arc model, *in* Soreghan, M.J., and Gehrels, G.E., eds., Paleozoic and Triassic Paleogeography and Tectonics of Western Nevada and Northern California: Geological Society of America Special Paper 347, p. 119–131, https://doi.org/10.1130/0-8137-2347-7.119.

Wernicke, B., and Klepacki, D.W., 1988, Escape hypothesis for the Stikine block: Geology, v. 16, p. 461–464, https://doi.org/10.1130/0091-7613(1988)016<0461:EHFTSB>2.3.CO;2.

Wolf, M.B., and Saleeby, J.B., 1995, Late Jurassic dike swarms in the southwestern Sierra Nevada Foothills terrane, California: Implications for the Nevadan orogeny and North American plate motion, *in* Miller, D.M., and Busby, C., eds., Jurassic Magmatism and Tectonics of the North American Cordillera: Geological Society of America Special Paper 299, p. 203–228, https://doi.org/10.1130/SPE299-p203.

Wright, J.E., 1982, Permo-Triassic accretionary subduction complex, south-western Klamath Mountains, northern California: Journal of Geophysical Research: Solid Earth, v. 87, p. 3805–3818, https://doi.org/10.1029/JB087iB05p03805.

Wright, J.E., and Fahan, M.R., 1988, An expanded view of Jurassic orogenesis in the western United States Cordillera: Middle Jurassic (pre-Nevadan) regional metamorphism and thrust faulting within an active arc environment, Klamath Mountains, California: Geological Society of America Bulletin, v. 100, p. 859–876, https://doi.org/10.1130/0016-7606(1988)100<0859:AEVOJO>2.3.CO;2.

Wright, J.E., and Wyld, S.J., 1986, Significance of xenocrystic Precambrian zircon contained within the southern continuation of the Josephine ophiolite: Devils Elbow ophiolite remnant, Klamath Mountains, northern California: Geology, v. 14, p. 671–674, https://doi.org/10.1130/0091-7613(1986)14<671:SOXPZC>2.0.CO;2.

Wright, J.E., and Wyld, S.J., 1994, The Rattlesnake Creek terrane, Klamath Mountains, California: An early Mesozoic volcanic arc and its basement of tectonically disrupted oceanic crust: Geological Society of America Bulletin, v. 106, p. 1033–1056, https://doi.org/10.1130/0016-7606(1994)106<1033:TRCTKM>2.3.CO;2.

Wright, J.E., and Wyld, S.J., 2006, Gondwanan, Iapetan, Cordilleran interactions: A geodynamic model for the Paleozoic tectonic evolution of the North American Cordillera, *in* Haggart, J.W., Enkin, R.J., and Monger, J.W.H., eds., Paleogeography of the North American Cordillera: Evidence for and against Large-Scale Displacements: Geological Association of Canada Special Paper 46, p. 377–408.

Wyld, S.J., 1991, Permo-Triassic tectonism in volcanic arc sequences of the western U.S. Cordillera and implications for the Sonoman orogeny: Tectonics, v. 10, p. 1007–1017, https://doi.org/10.1029/91TC00863.

Wyld, S.J., 2002, Structural evolution of a Mesozoic back-arc fold-thrust belt in the U.S. Cordillera: New evidence from northern Nevada: Geological Society of America Bulletin, v. 114, p. 1452–1468, https://doi.org/10.1130/0016-7606(2002)114<1452:SEOAMB>2.0.CO;2.

Wyld, S.J., Rogers, J.W., and Copeland, P., 2003, Metamorphic evolution of the Luning-Fencemaker fold-thrust belt, Nevada: Illite crystallinity, metamorphic petrology, and $^{40}Ar/^{39}Ar$ geochronology: The Journal of Geology, v. 111, p. 17–38, https://doi.org/10.1086/344663.

Yule, J.D., Saleeby, J.S., and Barnes, C.G., 2006, A rift-edge facies of the Late Jurassic Rogue–Chetco arc and Josephine ophiolite, Klamath Mountains, Oregon, *in* Snoke, A.W., and Barnes, C.G., eds., Geological Studies in the Klamath Mountains Province, California and Oregon: A Volume in Honor of William P. Irwin: Geological Society of America Special Paper 410, p. 53–76, https://doi.org/10.1130/2006.2410(03).